TORSION PENDULUM MEASUREMENTS ON VISCOELASTIC MATERIALS DURING VACUUM EXPOSURE

by Thomas C. Ward and Morris L. Evans

Prepared by
VIRGINIA POLYTECHNIC INSTITUTE AND STATE UNIVERSITY
Blacksburg, Va. 24061
for Langley Research Center

NATIONAL AERONAUTICS AND SPACE ADMINISTRATION • WASHINGTON, D. C. • JUNE 1972

1. Report No.	2. Government Accession No.	3. Recipient's Catalog No.
NASA CR-2074		

4. Title and Subtitle	5. Report Date
TORSION PENDULUM MEASUREMENTS ON VISCOELASTIC MATERIALS DURING VACUUM EXPOSURE	June 1972
	6. Performing Organization Code

7. Author(s)	8. Performing Organization Report No.
Thomas C. Ward and Morris L. Evans	
	10. Work Unit No.

9. Performing Organization Name and Address	11. Contract or Grant No.
Virginia Polytechnic Institute and State University Department of Chemistry Blacksburg, Va. 24061	NAS 1-10043
	13. Type of Report and Period Covered
12. Sponsoring Agency Name and Address National Aeronautics and Space Administration Washington, D. C. 20546	Contractor Report
	14. Sponsoring Agency Code

15. Supplementary Notes

16. Abstract

A torsional pendulum apparatus designed for testing in situ in vacuum, the dynamic mechanical properties of materials is described. The application of this apparatus to an experimental program to measure the effects of vacuum (10^{-5} torr) on the mechanical properties of two ablator materials (a foamed material and a filled elastomer) and a solid rocket propellant (a filled elastomer) is presented. Results from the program are discussed as to the effects of vacuum on the mechanical properties of these three materials. In addition, time-temperature-superposition, as a technique for accelerating vacuum induced changes in mechanical properties, is discussed with reference to the three materials tested in the subject program.

17. Key Words (Suggested by Author(s))	18. Distribution Statement
Vacuum effects on mechanical properties Ablator materials Solid propellants Accelerated testing of mechanical properties	Unclassified - Unlimited

19. Security Classif. (of this report)	20. Security Classif. (of this page)	21. No. of Pages	22. Price*
Unclassified	Unclassified	70	$3.00

*For sale by the National Technical Information Service, Springfield, Virginia 22151

TABLE OF CONTENTS

TORSION PENDULUM MEASUREMENTS ON VISCOELASTIC MATERIALS DURING VACUUM EXPOSURE

By Thomas C. Ward and Morris L. Evans
Virginia Polytechnic Institute and State University

I. INTRODUCTION

It has recently become apparent that polymeric-based materials may undergo significant mechanical property changes when exposed to vacuum environments[1]. In space flight, vacuum environments may be applied to a material for relatively long (years) periods. Catastrophic consequences may be projected for severe alterations in, for example, the modulus of a protective heat shield during space vacuum exposure. In view of the number of candidate materials to be screened for vacuum exposure effects and the required length of vacuum exposure, the need for a predictive (or accelerated) testing capability is also apparent.

Few methods exist to reliably perform in situ tests on the mechanical properties of polymeric samples when in vacuum environments[2]. In addition, accelerated testing procedures are far from well founded when vacuum induced changes are involved.

The purpose of the present investigation was to evaluate a torsion pendulum instrument designed for testing the dynamic mechanical properties of materials in vacuum. The evaluation was to focus on two points:

(1) Were vacuum induced changes detected over test periods of several days and what were they
(2) Could any induced changes be used to predict long-term vacuum effects on mechanical properties.

The sample temperature during vacuum exposure, the length of vacuum exposure, and the relative humidity conditioning of the materials prior to vacuum exposure were considered the important variables in this investigation.

Three materials were to be tested by the torsion pendulum while they resided in the vacuum environment:

(1) SLA 561v, and ablative heat shield
(2) TPH 3105, a solid propellant
(3) ESM 1004x, an ablative heat shield

---

1. Superscript numbers indicate references listed on page 36 and following.

II. LITERATURE REVIEW

A. Vacuum Induced Changes in Materials

Very little work has been reported concerning the effects of vacuum exposure on mechanical properties of materials, particulary on polymeric-based composites. The early investigations in this field are misleading because of poorly controlled test conditions. Later studies stressed the importance of *in situ* vacuum testing. Greenwood[1] has summarized most of the data reported on vacuum induced changes of elastomer-based propellant materials up to 1966.

In Greenwood's[1] experiments, solid propellant samples consisting of butadiene-acrylic acid binder and ammonium perchlorate (AP) oxidizer (very similar to that used in the subject investigation) were tested for ultimate modulus. The tests were conducted *in situ*, at ambient temperature, and with approximately 10^{-8} torr vacuum applied to the samples. It was found that the ultimate tensile strength increased by 29 percent after 4 days exposure, and by 60 percent after 32 days exposure. On the basis of mass spectrometric and weight loss data, Greenwood attributed the modulus change to a loss of water from the sample during the test. No quantitative relationship was established between the small water loss (only 0.15 percent in 400 hours) and the mechanical property changes.

Changes in the tensile stress-relaxation modulus of heat shield material SLA 561v during vacuum exposure (10^{-8} torr) at four temperatures were reported by Greenwood and Ward[3]. In three hours at 85° C as large as a 61 percent increase in modulus (compared to a control sample not under vacuum) resulted. However, Strauss[4] reported that similar vacuum exposures at ambient and for up to 96 hours had little effect on the tensile strength of SLA 561, an almost identical material to that used by Greenwood and Ward.

B. The Influence of Moisture Content on the Mechanical Properties of Polymers

Landel and Moser have done significant work concerning the effect of moisture on the dynamic mechanical properties of AP-polyurethane propellants[5]. There are strong chemical and physical similarties between the polyurethane and the poly(butadiene-*co*-acrylic acid) binder used in the TPH 3105 materials it should be noted. Landel and Moser discovered that:

(1) The modulus of the propellant was a sensitive function of its moisture content history; as much as a 100 percent increase in modulus was observed after a sample was maintained at 5°C and surrounded by 4.8 mm Hg partial pressure of water vapor for four days.
(2) Depending on the temperature, moisture exposure could raise or lower the propellant's modulus.

Landel and Moser suggested that multiple processes were at work in the propellant when its moisture content changed. Binder embrittlement and water plasticization of the binder were noted as two possible competing mechanisms involved.

Colodny and Ketchum[6] used tensile creep experiments at 31°C and 50°C to test moisture effects on polybutadiene based propellants. It was found that substituting an 80 percent R. H. sample environment for one at 0 percent R. H. decreased the sample modulus by as much as a factor of 8 after 100 hours of exposure.

Additional evidence of the influence of moisture content on moduli is available from Oberth and Bruenner[7]. Many examples can be found in the general polymer science literature to document the strong influence of varying amounts of water on the moduli of solid polymeric materials. In most cases[8] assumption that the water functions as a plasticizer is sufficient to account for mechanical property alterations. This is not always the case, however, particularly when the polymer in question is filled with an inorganic salt[9].

C. Accelerated Testing Procedures

For polymeric based materials, accelerated testing has been based on the time-temperature superposition principle (tTSP). The time dependent behavior of moduli prompted this theory. Since 1944, tTSP has been applied to homogeneous amorphous polymers with great success. Tobolsky[10] summarizes the evidence supporting tTSP and Ferry[11] discusses its applications in some detail. Basically, tTSP depends on the unimechanistic acceleration of molecular relaxations with increasing temperature in order to predict long time mechanical properties. In practice, modulus isotherms taken over short time periods are shifted along the time axis relative to a reference isotherm in order to produce a "master curve" extending over much longer times. The development of a rational for the isotherm shifts by Williams, Landel and Ferry[12] provided major impetus to the practice of tTSP.

Extention of the original tTSP procedures to a wide variety of physical properties of homogeneous polymers has been reported. In addition to stress-relaxation moduli, dynamic mechanical moduli, and creep compliances, the procedure has been applied to ultimate properties[13], and even to sliding friction coefficients[14]. Unfortunately, confirmations of the predicted properties in the form of actual long-term experimental data are virtually absent from the literature.

The time dependent mechanical properties of filled polymer systems, specifically elastomer-inorganic salt composites, have also been successfully analyzed by the tTSP[15,16]. It appears that as long as the polymeric binder dominates the material's stress-strain behavior, then tTSP is valid. Once again this validity is based on criteria other than long-time testing to confirm predicted moduli.

Drawing analogies with the tTSP, work has been done in which variables other than temperature have been used to accelerate mechanical property changes. These analyses depend on an empirical shifting of curves along a time axis to produce master curves much as was done with the isotherms in tTSP. Constant relative humidity[6,17] and high vacuum exposure[3] are two of the environmental conditions that have been used in superposition-type accelerated testing on polymeric materials. In both cases it was possible to obtain smooth master curves extending over long periods of time from short-time experiments under controlled conditions.

D. The Torsion Pendulum Method for Testing Mechanical Properties

Polymeric materials are viscoelastic; any test for material constants must take into account their time dependence. The torsion pendulum[18] offers a relatively simple way to determine the moduli in a dynamic test. The instrument has been successfully used on propellant-type materials[16]. These references revealed that the torsion pendulum was suitable for operation in a vacuum environment.

III. EXPERIMENTAL

A. Materials

(1) SLA 561v. This material was designed to be an ablative heat shield to protect spacecraft entering atmospheres of relatively low density (0.1 Earth atmosphere). Martin Marietta produced SLA 561v and has reported the following composition[19]:

Binder	poly(methyl, phenyl-siloxane)	
Filler (Wt. %)		
	Cork	29
	Silicone	25
	Fibers	5
	Phenolic microballoons ..	6
	Silica microspheres	35

(2) ESM 1004x. This composite was also designed as an ablative heat shield for atmospheres less dense than that of Earth. It was manufactured by General Electric Co. who reported[20] that it contained a binder of poly (methyl, phenyl-siloxane). A total of less than 50 Wt. % of filler was added to the binder. Iron oxide, silica and aluminum silicate fibers were used as the filler components. At room temperature ESM 1004x was sponge-like in texture; a high density of small open pores was apparent on the surface.

(3) TPH 3105. Thiokol Chemical Corporation made this solid propellant material. The binder was compounded from a butadiene-acrylic acid copolymer crosslinked with 0.84 Wt. % trispropyleneimine (MAPO) and cured in air for 64 hours at 135° F. The filler-oxidizer was AP having the following size distribution (based on Wt. % of final composite):

Passes through 200μ sieve	54.4%
Passes through 20μ sieve	24.6%

B. Test Apparatus

The torsion pendulum constructed for testing moduli of solid materials in vacuum is shown in Figures 1 and 2. The instrument is shown sitting inside a bell jar feed-through collar. In Figure 3 the apparatus is shown with the bell jar in place.

The torsion pendulum was designed to apply an oscillating shear torque to one end of a cylindrical test sample while holding the other end fixed. To achieve this the sample,

A, was attached between a freely oscillating inertia wheel, B, and a lower shaft, C, which could be locked into a fixed position (see Figures 1 and 2). A wire, D, Lever Arm, E, and weight pan, F, were used to counterbalance the inertia wheel and prevent any tensile stresses in the sample. The oscillatory motion was initiated via a rotary feedthrough, G, operating on a lever, H, attached to the lower shaft, C (see Figure 4).

In operation, a torque was applied to the sample through the lower shaft and the inertia wheel rotated in response. The initiator handle, I, was then used to lock the lower shaft back into its starting position, and the inertia wheel was left rotating restricted only by the sample which damped out its motion. A linear variable differential transformer (LVDT) core was attached to the outer rim of the inertia wheel, as shown in Figure 5, while the LVDT was held fixed as shown. The voltage signal from the LVDT went through an amplifier and filter, and was recorded on a oscillographic recorder.

The temperature of the entire apparatus was raised or lowered to roughly a few degrees below the desired sample temperature by blowing air and dry ice vapor into an insulated box which completely enclosed the bell jar and feed-through collar. This air-dry ice vapor mixture was supplied and temperature conditioned from a circulating gas controller. Once this approximate temperature control was established, the heating coils, J, seen in Figure 6, were used to fine control the sample temperature. These heating coils were made of a length of nichrome resistance wire wound around two cylindrically shaped glass spools. These spools were placed such that the sample was centered inside of one spool while a dummy sample, K, was centered inside the other. The resistance wire was connected to a variable transformer which in turn was connected to a temperature sensor-controller. The dummy sample was identical to the actual sample except it was drilled axially so as to allow emplacement of a bead thermister in its center. Powder from the drilling was packed back into the hole of the dummy sample after the thermister was placed. The thermister was connected to the temperature sensor-controller which had strip-chart recording capability. In this way, a continuous measure of the dummy sample temperature was obtained, and precise temperature control of the real sample was realized. A precision of $\pm$ .02°C was obtained for all except the 5°C runs. The 5°C runs were controlled to $\pm$ .2°C.

The pumping station was of conventional design; a 6 inch oil diffusion pump was backed up by a standard

mechanical forepump. A liquid nitrogen trap protected the bell jar from pump oil contamination. Pressures of 5×10^{-5} torr, measured by a calibrated ionization gage and controller, could be achieved in 30 minutes with this system.

C. Sample Preparation and Preconditioning

Samples of each of the three materials were cut from the center of single, large blocks of that material. They were cut from the same block face each time. A thin wall stainless steel borer was used to core out these cylindrical rod shaped samples which averaged about 0.8 cm diameter. The rods were then cut to about a 7 cm length with a razor blade. An epoxy resin (Type A1, Armstrong Products Co., Warsaw, Ind.) was used to glue flat aluminum discs to the sample ends. A jig was used in the glueing process to insure that the two discs were centered and parallel to one another. Holes were drilled in the perimeter of the discs to allow for mounting in the torsion pendulum. Figure 7 shows a sample ready for testing.

Each sample was preconditioned at a designated relative humidity and at room temperature for a minimum of two weeks. The proper relative humidity atmospheres were achieved by water-glycerin solutions placed in the bottom of air-tight desiccators[21]. Glued-up samples were placed on shelves above the solutions. All of the ESM 1004x and SLA 561v samples were preconditioned at 50 percent R. H. Three TPH 3105 samples were preconditioned at 50 percent, two at 25 percent, and two at 75 percent R.H.

D. Test Procedure

On removing a sample from the proper preconditioning dessicator, the time required to mount the samples and align all of the complimentary components of the torsion pendulum was approximately one hour. After this an additional half hour was needed to pump the system down to the test pressure, and achieve temperature control. Temperature control of the sample was established as soon as the bell jar pressure reached the 10^{-5} torr range.

When a sample was mounted and still at ambient temperature and pressure, the torsion pendulum was activated as described above and the output recorded for later analysis. The bell jar was then pumped out as quickly as possible. The zero of vacuum exposure time was noted when 1×10^{-4} torr was reached. A data point was taken at this time.

Intervals of 15 to 30 minutes separated the data points on the first day of a test run. A minimum of about 1000

seconds was required between points in order for the inertia wheel to come to rest prior to activating the torsion pendulum. On suceeding days a period progressing from an hour to 5 or 6 hours separated data points. Typically, about 30 data points might be obtained during a 4 day test run.

Samples of SLA 561 and TPH 3105 each underwent tests of ninety-six hours vacuum exposure time at 45° C, 25° C, and 5° C. ESM 1004x, in addition to these temperatures, underwent a test at 80° C. The samples of TPH 3105 which were preconditioned at 25 percent and 75 percent relative humidity were subjected to vacuum exposure for ninety-six hours at 25° C. Logs of the temperature and pressure inside the bell jar were kept during all of these runs.

IV. DATA REDUCTION

A. Calculation of the Moduli

A reproduction of a recorder trace obtained during a typical torsion pendulum experiment is shown in Figure 8. The characteristic damped sine wave which appears may be analyzed in terms of the frequency of the oscillation, ω, and the damping, expressed as the amplitude ratio A_1/A_2.

The formulas used for the calculations are essentially the same as those used by Nielsen[18] and others[11]:

$$G' = \frac{\omega^2 I}{b} \tag{1}$$

$$b = \frac{\pi r^4}{2L} \tag{2}$$

$$G'' = \frac{G'}{\pi} \ln \frac{A_1}{A_2} \tag{3}$$

$$G^* = \sqrt{(G')^2 + (G'')^2} \tag{4}$$

ω = frequency of output, radians/sec
I = moment of inertia of wheel, gr cm^2
r = sample radius, cm
L = sample length, cm
A_1 = amplitude of wave "n"
A_2 = amplitude of wave "n + 1" (see Figure 8)
b = shape factor, cm^3
G* = complex modulus, dynes/cm^2
G' = storage modulus, dynes/cm^2
G" = loss modulus, dynes/cm^2

and the complex modulus, G*, is seen to have two contributors: the storage modulus, G', and the loss modulus, G". Equations 1 - 4 are applicable when the material under analysis is linearly viscoelastic (for discussion of this see reference 10) and when G" < G'. In particular, the full equation for G' is [18]:

$$G' = \frac{I W^2}{b} \left[1 - \frac{1}{4\pi^2} \left(\ln \frac{A_1}{A_2} \right)^2 \right] \tag{5}$$

The $\frac{1}{4\pi^2} \left(\ln \frac{A_1}{A_2} \right)$ term has been neglected in our storage modulus calculation because it is negligibly small. It is on the order or 0.0016 when compared to one when typical amplitudes obtained in the present work are substituted.

B. Analysis of Vacuum Exposure Effects.

An empirical equation was used to fit the isothermal modulus as a function of vacuum exposure time data obtained in this work. The equation is:

$$\log G = I + n(B-3) + d \tanh\left(\frac{B-B_c}{B}\right) \qquad (6)$$

where G can be either the storage or the loss modulus, I is log of G at 1000 seconds of vacuum exposure, B is the log of the vacuum exposure time expressed in seconds, n is the slope of the linear line segement extenting from B = 3 to some exposure time $B=B_c$, and d is a constant equal to zero if $B < B_c$ and equal to 0.405 if $B > B_c$. This equation was not chosen from theoretical considerations but because it was found to provide an adequate representation of the data.

V. RESULTS AND DISCUSSION

A. General Comments on the Accuracy, Precision and Interpretation of the Results.

Test for Linearity

Linear viscoelastic behavior had to be established for each of the three test materials. Equations 1-4 are not valid for non-linearly viscoelastic solids and non-linear analysis is extremely difficult. A sample of each material at 25°C was subjected to a number of shear strains up to 5.23×10^{-3} radian per cm length, approximately twice the strain level used in the standard testing procedure. In all cases the calculated moduli were identical and independent of strain. This constitutes sufficient proof of linear viscoelastic response.

Precision

The precision (reproducibility) of the modulus measurements was determined for each of the three test materials. This was accomplished by comparing results obtained on several identically prepared and tested samples of each material. These comparative tests were run at atmospheric pressure, no vacuum having been applied to the samples. Detailed results are presented in Appendix A. Summarized, the results indicate good reproducibility. The complex moduli were as follows:

MATERIAL	RANGE OF G*, EXPRESSED AS % OF THE MEAN VALUE
ESM 1004x	5.10
SLA 561v	2.51
TPH 3105	0.436

Two data readings were made at each vacuum exposure time during an experiment. The greatest complex modulus difference between these two which was observed in each case was divided by the mean of the two moduli in order to get the ranges listed above. Further comments on precision may be found in the Error Analysis section.

Accuracy

The accuracy of the torsion pendulum instrument was checked by comparison of its data on SLA 561v with that of The National Bureau of Standards on the same material[22]. Appendix B lists the test conditions and results in detail. Briefly, the complex moduli obtained in the subject work were within 4% of the NBS values. This certainly indicates that the torsion pendulum equipment was functioning properly and that the data analysis was correct.

The Error Analysis section contains quantitative comments on the accuracy of the moduli determinations from sample to sample.

Interpretation

Since the results are presented below in terms of G', G", and G*, a brief discussion of these moduli follows.

The time dependence of moduli of viscoelastic materials indicates that both strain and rate of strain must be considered in testing[10,11]. Strain contributes to the modulus in a time independent or elastic way; Young's modulus is an example. Strain rate contributes to the modulus because of the material's resistance to viscous flow. Strain and strain rate contributions to the total, or complex, modulus (G*), are denoted by G' and G" respectively in a dynamic shear test. The elastic component, G', is a measure of the energy stored in the material during one cycle in the dynamic test[8]. Conversely, G" measures the dissipation of energy per cycle and is manifested as the damping effect in the torsion pendulum type of dynamic test[8].

B. The ESM 1004x Material

Results

All of the ESM 1004x samples were preconditioned at 50% R. H. as described in the experimental section. Figures 9 and 10 show the dependence of the isothermal storage and loss moduli on vacuum exposure time. The bell jar pressure in all cases was 5×10^{-5} torr or less. A pressure-time history for each run has been provided in Appendix C. The complex modulus data coincide to better that 1% at all points with the storage modulus and so are not shown separately.

The influence of temperature on the moduli of ESM 1004x is shown in Figures 11 and 12. All these data were obtained at atmospheric pressure.

Storage Modulus Discussion

In the 5° C - 80° C temperature range, very little change appears in G' during the four day vacuum exposure. Figure 10 illustrates that, within the precision of these results, G' of ESM 1004x is predicted to remain constant under the imposed test conditions and preconditions. At 8° C only, analysis of the data shows a possible increase of 5-8% in G', too close to the experimental error of±2% to be regarded as conclusive evidence of a change. These data thus indicate that in static applications (no change in strain) the modulus of 50% R. H. preconditioned ESM 1004x is stable to vacuum exposures of about 5×10^{-5} torr for four days.

The order G' (80° C) > G' (5° C) > G' (45° C) > G' (25° C) was unexpected (see reference 10 for a discussion of the temperature dependence of rubbery materials). Figure 12 shows that for a single sample the temperature dependence of G' was slight and similar to that usually found for elastomers[10]. This indicated the sample-to-sample variation for this material was large (see Error Analysis section) even though the relative values were rather precise. Due to the numerous large pores and the ill-defined boundries of samples of this material this fluctuation is not surprising. Equations 1-4 show that

G' depends on the forth power of the sample radius, and thus, dimensional uncertainties are magnified in the moduli calculations.

Loss Modulus Discussion

Significant decreases in G" occurred during the vacuum exposure. This is illustrated in Figure 13 which shows, on an enlarged scale, least squares regression lines determined from the same data plotted in Figure 10. The absolute values of the isotherms are, as discussed above , not as expected. But, the slopes of the lines indicate a steadily increasing rate of G" degradation with temperature increase. This dependence is summarized in Figure 14.

At 80° C a 25.5% decrease of G" occurred after the four day vacuum exposure. This could be quite serious if ESM 1004x was used in applications where high strain rates were applied and the material was accordingly tested.

Accelerated Testing Discussion

No superposition scheme was found that would work on the data for ESM 1004x. For G' this was simply because there was no change detected that was large enough to accelerate. In the case of G", the straight lines of Figure 13 may be extrapolated to long times. Alternatively, the equation

$$\log \left[G''(t) / G''(t=0) \right] = n' \log t \qquad (7)$$

where G"(t=0) is the experimentally determined loss modulus prior to vacuum exposure, t is the vacuum exposure time in seconds, and n' is obtained from Figure 14, can be used to predict the loss modulus after long vacuum exposures.

C. The SLA 561v Material

Results

All the data taken on SLA 561v came from samples pre-conditioned at 50% R.H.. The complex, storage, and loss moduli isotherms are shown in Figures 15, 16 and 17 as functions of vacuum exposure time. Runs were made with the samples thermostated at 5° C, 25° C, and 45° C. Pressure-time histories for each of the three runs are listed in Appendix D. These histories indicate that pressure environments of 5×10^{-5} torr or less existed during all the runs.

Sample to sample variation in the data was small for SLA 561v. The sample dimensions were unambiguous and easily measured. Hence, as discussed in detail in the Error Analysis section, the absolute values of the moduli in each run should be relatively accurate.

Storage Modulus Discussion

No change was observed in G' during the vacuum exposure of four days. Figure 16 shows that when a double logarithmic plot of G' vs. vacuum exposure time was made, straight lines of slope zero resulted at all three test temperatures. The relative ordering of the moduli in which the 5° C modulus was highest and the 45° C modulus was lowest was consistent with previous reports[19].

These G' results should be compared with the data of Greenwood and Ward[3] who found that vacuum produced a definite increase in the stress-relaxation modulus, E_r, of SLA 561v. Since their tests were run at zero strain rate (by definition of the stress-relaxation modulus) then E_r and G' should be directly proportional to one another[8]. The most apparent explanation for the discrepancy between the observations comes from the fundamental difference in the two types of test involved. In a stress-relaxation experiment the sample is continuously subjected to a fixed imposed strain throughout the test period. However, the dynamic test as employed in the subject work applies strain only intermittantly to the sample. Thus, states of strain exist in the sample less than 0.1% of the total test time. Should vacuum induced changes in SLA 561v depend on non-zero strain states existing in the test sample, then Greenwood and Ward's experiments would have detected modulus variations whereas none would have been seen in the present work.

Loss Modulus Discussion

The discussion of the G" results is very similar to that for G'. Figure 17 reveals that SLA 561v's loss modulus was essentially independent of vacuum exposure time over the four day test. This observation was true over the 40° C temperature range investigated.

Accelerated Testing Discussion

Within the imposed experimental conditions no detectable vacuum induced changes occured in G' or G" (and hence in G*). SLA 561v was indicated to be a very stable material with respect to its mechanical integrity during vacuum exposures and small sample deformations. It follows that there was nothing in the data to which any accelerated testing technique might be applied.

D. The TPH 3105 Material

Results

The effects of vacuum exposure on the moduli of 50% R.H. preconditioned TPH 3105 are shown in the isotherms plotted in Figures 18, 19 and 20. Pressure-time histories for these runs are given in Appendix E; these show that environments of 5×10^{-5} torr or less were applied to the samples during testing.

The consequences of varying the preconditioning R.H. were also examined for TPH 3105. Figures 21,22 and 23 show the moduli-vacuum exposure time 25^{o} C isotherms for samples subjected to 25%, 50% and 75% R.H. preconditioning. Appendix F contains the appropriate pressure-time histories which reveal that 5×10^{-5} torr or less of vacuum was applied to the samples during these runs.

As previously presented, the precision of the data for TPH 3105 was about 0.5%. There was little uncertainty associated with the sample dimensions, and no visible or viscoelastic signs of dewetting of the filler-binder interface were found. In addition, there was no apparent color change at any stage of the preparation or testing of TPH 3105.

Storage Modulus Discussion

This discussion is confined to those samples preconditioned at 50% R.H.. Figure 19 shows that G' increased with increasing vacuum exposure. The resulting 5^{o} C, 25^{o} C and 45^{o} C isotherms are very similar in shape. In the initial stages of vacuum exposure, Figure 19 illustrates a linear relationship between log G' and the logarithm of vacuum exposure time. During the final 3.5 or so days of the test a curved relationship is found as shown. Figure 24 contains a replot (25^{o} C isotherm only) of the data from the curved region appearing in Figure 19. The linear scale used in Figure 24 makes it clearer that G' asymptotically approached a limiting value during the test run. This limiting value represented an increase in G' of 23%, 37% and 31% at 5^{o} C, 25^{o} C and 45^{o} C, respectively.

The storage moduli of viscoelastic materials have frequently been observed to increase on loss of low molecular

weight "plasticizing" diluents[23]. Dehydration of the butadiene-acrylic acid copolymer used as a binder for TPH 3105 could easily have been responsible for the observed modulus increase. Whatever the cause, the material was elastically "stronger" in resisting small deformations after its vacuum exposure of four days.

Loss Modulus Discussion

Only the data from samples preconditioned at 50% R. H. are discussed in this section. Figure 20 shows that the TPH 3105 loss modulus behavior in vacuum environments paralleled that of the storage modulus. The 25° C isotherm in Figure 25 suggests the same asymptotic characteristic for G" as was observed in the storage modulus case. The asymptotes approached by G" gave rise to 36%, 56% and 54% increases in the loss modulus at 5° C, 25° C and 45° C, respectively.

For homogeneous polymeric materials the loss and storage moduli usually are observed to change in opposite directions when environmental parameters are altered[8]. For composites such as TPH 3105, however, the opposite tendency has sometimes been observed[5]. There are several possible explanations consistent with this behavior:

(1) An alteration of the binder microstructure (see reference 5) might have been involved. This is thought to be caused by partial dissolution of the salt (AP in the case of TPH 3105) into the binder. This consequently raises the internal viscosity of the binder's polymeric network and, hence, the contribution of G".

(2) The binder-filler interface might have been altered both geometrically and with respect to intermolecular forces. The internal resistance to flow as measured by G" would thus be modified.

(3) There might be competing mechanisms of some kind initiated by the vacuum exposure. One of these might influence G' and the other, G".

Summarizing the loss modulus behavior, the exposure of TPH 3105 to vacuum was found to significantly increase G' by the end of a four day exposure. The material was thus better able to absorb energy in a deformation and correspondingly less "brittle".

Preconditioning Effects Discussion

Different preconditioning environments clearly altered the TPH 3105 propellant's viscoelastic properties. Figures 22 and 23 show that at 25° C the initial (pre-vacuum exposure) loss and storage moduli were increased by 32.4% and 46.0% respectively when the preconditioning R.H. was lowered from 75% to 25%. Figures 26 and 27 present the initial modulus-R.H. relationship in linearized form.

Inspection of Figure 22 suggests that the three storage

moduli represented there converged toward a common isotherm at the longer vacuum exposures. This was not so for the loss modulus according to Figure 23. Only for G' were the effects fo varying preconditionings lessened by the vacuum environment. This evidence supports explanation (3) above because it implies multiple mechanisms were involved in the changes in TPH 3105.

Accelerated Testing Discussion

The data on TPH 3105 were found to be nonsuperimposable; they could not be used to construct a master curve of the tTSP type. Similarly, attempts to superimpose the data using the preconditioning R.H. as the independent variable instead of temperature were not successful. A variety of linear, logarithmic and semi-logarithmic plots were made in these unsuccessful efforts to expand the time scale of vacuum exposure.

In lieu of superposition methods an analytic technique was applied to accelerated testing of TPH 3105. Equation 6 was used to represent the data shown in Figures 18-23. Constants of the equation were empirically adjusted for each isotherm and preconditioning in order to obtain an accurate fit to the data over the entire test period. These constants are listed in Appendix G. The agreement between moduli calculated using Equation 6 and the actual experimentally determined moduli was quite good; they were within 0.020 log unit of each other over most of the four day vacuum exposure (see Appendices H and I for detailed comparisons).

To make predictions concerning the long time ($>$ 4 days) moduli of TPH 3105 based on the data of the subject work, first the appropriate temperature and preconditioning R.H. must be used to identify the three constants I, n, and B_c of Equation 6. Figures 28, 29 and 30 were prepared to aid in this selection. Having the correct constants, a substitution of the log of some vacuum exposure time, B, into Equation 6 yields the predicted modulus.

VI. ERROR ANALYSIS

Equations 1-3 were used to calculate the viscoelastic moduli from the raw data. For convenience these equations are repeated:

$$G' = \frac{w^2 I}{b} \tag{1}$$

$$b = \frac{\pi r^4}{2L} \tag{2}$$

$$G'' = \frac{G'}{\pi} \ln \frac{A_1}{A_2} \tag{3}$$

Errors have been evaluated by using Equations 1-3 and by estimating limits for the various observable parameters. This was done by assigning error bands based on multiple observations of the data. A full statistical treatment was not possible given the small populations and observations involved. In general, unless mentioned otherwise below, the error interval ($\pm$ limit) was assigned in accordance with what was approximated to be $\pm$ one standard deviation (normal distribution) about the mean value.

A. Errors Applying to All Three Materials

The Moment of Inertia Error

Equation 1 contains a parameter I, the moment of inertia of the rotating wheel (without the attached sample) of the torsion pendulum. This was determined from a calibration using the equation

$$I_w = I_r \frac{W_r^2}{W_w^2} \tag{8}$$

where:

I_w = moment of inertia of wheel and attached sample, g/cm^2

W_w = natural frequency of oscillation of above wheel mounted in torsion pendulum, radians/sec

W_r = natural frequency of oscillation of a steel cylindrical rod mounted in torsion pendulum of above wheel, radians/sec

I_r = moment of inertia of above rod, g/cm^2

= 1/12 (mass)(length)^2

Assigning error limits based on the maximum observed deviation from the mean value gives:

$$\text{mass} = 35.9725 \pm 0.0005 \text{ g}$$
$$\text{length} = 14.618 \pm 0.005 \text{ cm}$$
$$W_r = 0.1155 \pm 0.0005 \text{ rad/sec}$$
$$W_w^r = 0.006255 \pm 0.000005 \text{ rad/sec}$$

Substitution into Equation 8 gives

$$I_w = 2.204 \times 10^5 \pm 2.5 \times 10^3 \text{ g/cm}^2$$

Thus, a maximum uncertainty of about 1% entered into the absolute value of the moduli through the I_w error. This error was constant for all runs reported in the subject work.

Amplitude and Frequency Measurement Errors

An examination was made of a number of duplicate oscillographic recorder traces (see Figure 8) which represented the raw data coming from the torsion pendulum voltage output. It was observed that frequency could be determined to about 0.0015 cycle per second in 1 cycle per second. Amplitudes were reproducible to about 1.2 chart units in 100 chart units. Substitution of these error limits and typical numbers for I, b, and w into Equations 1 and 3 showed that about 1% error was introduced in G' and about 3.3% variation appeared in G". These were responsible for the principle point to point modulus fluctuations during any single run.

Errors Introduced by Temperature and Pressure Fluctuations

Sample temperature was controlled to $\pm 0.02^{\circ}$ C during a run. In order to estimate the effect of this fluctuation on the modulus, Figure 11 was used. It was assumed that ESM 1004x was typical of all three materials in its modulus-temperature behavior. A slope, dG'/dT, of 3.13×10^2 dyne/cm^2 deg was determined as an average value at various points on the curve in Figure 11. Using this coefficient and the $\pm 0.02^{\circ}$ C variation in temperature, it was calculated that ± 6.26 dynes/cm^2 of error in the storage modulus could thereby be introduced. Using Figure 12, the loss modulus fluctuation due to inprecise temperature control was found to be smaller than that for the storage modulus. Both are clearly insignificant errors.

To determine the effect of a pressure change on the materials, moduli values were calculated for data taken at various pressures between 1×10^{-4} and 5×10^{-7} torr. This was done for each material. The effect of the pressure change on both G' and G" values was found to be negligible for each material.

B. Errors Specific for a Particular Material

These errors arose from uncertainties in the sample dimensions. During any particular run the relative values of calculated moduli were unaffected by these errors. However, from sample to sample (and a new sample was used in each run) the dimensional error entered the calculations.

Equation 2 defines the shape factor b which is seen to depend on the sample size. Raising the sample radius, r, to the fourth power, as Equation 2 demands, means that any error in r will be greatly magnified in the calculated moduli.

ESM 1004x Material

The largest errors in the subject work occurred in determining the dimensions of ESM 1004x. The materials irregular surface boundaries caused the radius determination to be known only to within $\pm$ 0.0075 cm (estimated from multiple readings) in a radius about 0.485 cm. The sample length was determined to $\pm$ 0.010 cm over a 6 cm total (similarly estimated). Accordingly, the absolute value of G' and G" calculated from Equations 1-3 varied by $\pm$ 8.1% due to the combined radius and length errors.

TPH 3105 and SLA 561v Materials

Because of the smooth and well defined surfaces of these samples, their radii were measured to $\pm$0.00325 cm in about 0.395 cms total. The length determination error was the same as for ESM 1004x above, i.e., $\pm$ 0.01 cm over a 6 cm length. Combining the two produced a $\pm$ 2.82% variation in G' and G".

C. Summary of Error Analysis

Regarding the various individual errors discussed above as independent, and adding them together where appropriate, the following approximate assignments were made:

(1) Errors in Absolute Values of Moduli

ESM 1004x	.....	G' = $\pm$ 9%
		G" = $\pm$ 9%
SLA 561v	.....	G' = $\pm$ 4%
		G" = $\pm$ 4%
TPH 3105	.....	G' = $\pm$ 4%
		G" = $\pm$ 4%

(2) Error in the Relative Moduli

All three materials ... G' = $\pm$2%
G" = $\pm$4%

VII. CONCLUSIONS

The following conclusions were drawn from the results of this investigation:

1. The torsion pendulum was a sensitive and accurate instrument for monitoring the complex modulus of polymeric materials during vacuum exposures of about 5×10^{-5} torr.

2. Accelerated testing of vacuum induced changes in in moduli of ESM 1004x and TPH 3105 could not be done using time-temperature superposition concepts. However, moduli predictions were made based on analytical extrapolations of trends in the data.

3. No change was detected in the shear moduli of SLA 561v obtained by intermittant testing during a four day vacuum exposure.

4. The storage modulus of ESM 1004x increased by 8% and the loss modulus decreased by 38% on exposure of the material to vacuum of about 5×10^{-5} torr for four days at 45° C. Lower temperatures produced smaller changes.

5. The storage modulus of TPH 3105 increased about 37% and the loss modulus increased about 56% on exposure of the material to vacuum of approximately 5×10^{-5} torr for four days at 25° C. Tests at 5° C and 45° C produced smaller changes.

6. The TPH 3105 propellant's mechanical properties were very sensitive to preconditioning relative humidities.

VIII. RECOMMENDATIONS

Based on the results of this investigation, the following recommendations for future work are suggested:

(1) Determine the moduli of TPH 3105 and other polymeric composites over long vacuum exposure times (order of months). These data are greatly needed for checking predictive testing results.

(2) Investigate potential moduli changes during simultaneous application of small tensile strains (with a continuous loading pattern) and vacuum environments to samples of SLA 561v.

(3) Determine the relative importance of filler, binder, and interfacial effects in vacuum induced moduli changes in propellant type materials. A systematic variation of sample composition combined with vacuum measurements would provide a start in this investigation.

APPENDIX A

Reproducibility of the Torsion Pendulum Data

Moduli listed below were calculated from data on samples preconditioned at 50% R. H. All the moduli were determined at 1 atmosphere and at the indicated temperatures. No vacuum had been applied to these samples at the time of these tests.

MATERIAL	SAMPLE NO.	G', dynes/cm^2	G", dynes/cm^2	G*, dynes/cm^2
ESM1004x 45° C	1	9.719×10^5	3.233×10^4	9.725×10^5
	2	10.23×10^5	3.162×10^4	10.23×10^5
SLA 561v 25° C	1	1.054×10^8	1.271×10^7	1.062×10^8
	2	1.054×10^8	1.300×10^7	1.062×10^8
	3	1.082×10^8	1.233×10^7	1.089×10^8
TPH 3105 25° C	1	7.047×10^7	7.517×10^6	7.087×10^7
	2	7.077×10^7	7.571×10^6	7.118×10^7
TPH 3105* 25° C	1	5.390×10^7	6.636×10^6	5.430×10^7
	2	5.390×10^7	6.473×10^6	5.430×10^7
	3	5.390×10^7	6.345×10^6	5.430×10^7
	4	5.390×10^7	6.583×10^6	5.430×10^7

* preconditioned at 75% R. H.

APPENDIX B

Comparison of SLA 561v Results with NBS Test on SLA 561v

To access the absolute accuracy of the moduli obtained by the torsion pendulum developed in this work, comparison was made with data obtained by the National Bureau of Standards (NBS). A sample of SLA 561v identical in all respects to those used in this study was preconditioned for one month at 25° C and 50% R. H. and then taken to the NBS Labs for testing. The sample was continuously kept at 50% R. H. until immediately before the test, which took only a few minutes. The NBS tests were performed on a Weissenberg Rheogoniometer at 25° C and the results are as follows (along with results from this study on the initial moduli of SLA 561v).

Instrument	G', dynes/cm^2	G", dynes/cm^2
Torsion pendulum	1.00×10^8	1.21×10^7
NBS Rheogoniometer	9.6×10^7	1.00×10^7

Tests on the Rheogoniometer were run at 0.25 Hz, very close to the nominal 0.24 Hz frequency of the torsion pendulum.

The agreement above is considered excellent in view of the fact that the loss modulus G" is difficult to determine on the rheogoniometer when G' $>$ G" by a factor of 10.

APPENDIX C

Pressure-time Histories for ESM 1004x Runs.

All samples were preconditioned at 50% R. H. P = bell jar pressure, torr; B = log of the vacuum exposure in seconds.

5° C		25° C		45° C		85° C	
B	Px10^5	B	Px10^5	B	Px10^5	B	Px10^5
2.9817	2.5	2.8866	4.2	2.7782	3.7	3.0080	5.9
3.2689	2.4	3.1393	4.2	3.4314	3.0	3.3216	5.9
3.4496	2.2	3.3572	4.1	4.3904	2.0	3.4935	4.9
3.5556	2.8	3.5257	4.6	4.6029	1.9	3.6100	4.7
3.7268	2.0	3.6287	4.0	4.7177	1.9	3.8566	4.2
3.8638	1.8	3.7219	3.6	4.7910	1.9	3.9109	3.9
3.9564	2.2	3.7860	3.6	4.8235	1.9	4.0078	3.5
4.0278	2.2	3.8566	3.5	4.8768	1.4	4.0584	3.9
4.1016	1.8	3.9564	3.5	4.8954	1.4	4.5882	2.3
4.1539	1.8	4.0053	3.5	4.9279	1.2	4.6046	2.2
4.1890	1.9	4.0515	3.4	4.9359	1.2	4.6255	2.0
4.2879	1.7	4.1118	3.4	4.0953	1.0	4.7880	1.5
4.3062	1.4	4.1647	3.8	5.1004	1.0	4.8952	1.2
4.4067	1.6	4.2198	3.4	5.1370	1.0	4.9202	1.2
4.4178	1.6	4.2673	3.4	5.1464	1.0	5.0178	1.0
4.7334	0.6	4.3432	3.5	5.2108	1.1	5.0020	1.0
4.7401	0.58	4.3594	3.4	5.2151	1.2	5.1445	1.1
4.8710	1.0	4.4088	3.4	5.2003	1.2	5.1508	1.0
4.8755	1.0	4.4188	3.4	5.3105	1.2	5.2455	1.0
4.9593	0.52	4.7997	3.4	5.3133	1.2	5.2492	1.0
4.9659	0.56	4.8078	3.4	5.3345	1.3	5.3598	1.0
5.0481	0.38	4.8151	3.4	5.3383	1.2	5.3642	1.0
5.0509	0.37	4.9218	2.8	5.3458	1.2	5.3661	1.0
5.1793	0.47	4.9271	2.6	5.3520	1.2	5.4750	1.0
5.1817	0.38	5.0178	1.8	5.4741	3.1	5.4795	1.0
5.2687	0.28	5.0222	1.7	5.4814	3.1	5.4836	1.0

APPENDIX C, CONT.

5° C		25° C		45° C		85° C	
B	$Px10^5$	B	$Px10^5$	B	$Px10^5$	B	$Px10^5$
5.2714	0.29	5.1983	1.6	5.4836	3.2	5.5360	1.0
5.3927	0.30	5.2004	1.6	5.5806	4.0	5.5372	1.0
5.3963	0.28	5.2830	1.9	5.5826	4.0	5.5388	1.0
5.5038	0.10	5.2849	2.0	5.5912	3.9		
5.5053	0.10	5.3873	2.0	5.6730	2.4		
5.5372	0.92	5.3885	2.0	5.6762	5.1		
5.5388	0.89	5.4541	1.6	5.6779	5.1		
		5.4552	1.6	5.7532	5.4		
		5.5171	1.8	5.7584	5.2		
		5.5192	1.9	5.8682	8.0		
		5.5378	1.7	5.8693	8.0		
		5.5391	1.8	5.8830	8.0		
				5.8865	7.7		
				5.8872	7.4		

APPENDIX D

Pressure-time Histories for SLA 561v Runs

All samples were preconditioned at 50% R. H. P = bell jar pressure, torr; B = log of the vacuum exposure time in seconds.

5° C		25° C		45° C	
B	Px10^5	B	Px10^5	B	Px10^5
3.1755	9.5	3.0563	4.3	3.0786	6.1
3.2089	9.5	3.0998	4.2	3.1200	6.1
3.3216	8.6	3.3216	4.0	3.3216	5.9
3.3457	8.6	3.3457	4.0	3.3457	5.9
3.4935	9.2	3.4935	3.8	3.5017	5.7
3.5099	9.2	3.5099	3.8	3.5099	5.7
3.6100	9.2	3.5904	3.8	3.6226	5.6
3.6226	9.2	3.6100	3.8	3.6348	5.6
3.7687	8.9	3.7069	3.8	3.7774	5.4
3.7774	8.9	3.7170	3.8	3.7860	5.4
3.8880	8.9	3.8493	3.6	3.8913	5.3
3.8947	8.9	3.8566	3.6	3.8980	5.3
4.0374	9.0	3.9788	3.6	4.0561	5.3
4.0422	9.0	3.9842	3.6	4.0607	5.3
4.1890	8.6	4.1198	3.7	4.2260	5.3
4.2214	8.6	4.1237	3.7	4.2291	5.3
4.3276	8.7	4.3865	3.4	4.3276	5.3
4.3288	8.7	4.2892	3.4	4.3300	5.3
4.4208	8.7	4.4512	3.3	4.4666	5.3
4.4227	8.7	4.4540	3.3	4.4684	5.3
4.4999	8.6	4.5437	3.4	4.5626	5.2
4.5032	8.6	4.5452	3.4	4.5640	5.2
4.6765	8.6	4.8387	3.4	4.6465	5.3
4.6776	8.6	4.8394	3.4	4.6477	5.3
4.7968	8.2	4.9533	3.3	4.8650	5.5

APPENDIX D, CONT.

5° C		25° C		45° C	
B	$Px10^5$	B	$Px10^5$	B	$Px10^5$
4.7988	8.2	4.9536	3.3	4.8657	5.5
4.9243	7.9	5.0509	3.4	4.9670	5.6
4.9258	7.9	5.0516	3.5	5.9681	5.6
5.0377	7.2	5.1876	3.2	5.0509	5.8
5.0385	7.2	5.1878	3.2	5.0537	5.8
5.1825	1.0	5.2902	3.3	5.2043	6.1
5.1827	1.0	5.2905	3.3	5.2047	6.1
5.3422	0.41	5.4223	3.4	5.3899	6.0
5.3428	0.40	5.4225	3.4	5.3903	6.0
5.3439	0.39	5.5137	4.7	5.3907	6.0
5.3449	0.40	5.5139	4.7	5.4770	6.3
5.4539	0.38	5.5375	3.2	5.4771	6.3
5.4547	0.38	5.5377	3.2	5.4773	6.3
5.4549	0.38			5.5198	6.3
5.5375	0.34			5.5200	6.3
5.5376	0.34			5.5214	6.3
5.5378	0.35			5.5375	6.6
5.5378	0.35			5.5379	6.6

APPENDIX E

Pressure-time Histories for TPH 3105 Runs.

All the samples were preconditioned at 50% R. H. P = pressure in torr; B = log of the vacuum exposure time in seconds.

5° C		25° C		45° C	
B	Px10^5	B	Px10^5	B	Px10^5
3.0328	1.0	3.1200	1.0	0.6971	0.30
3.0786	1.0	3.1393	1.0	3.0328	0.16
3.3216	0.58	3.2827	0.86	3.0786	0.16
3.3457	0.58	3.2960	1.0	3.2960	0.13
3.5017	0.45	3.4402	0.78	3.3216	0.13
3.5178	0.45	3.4587	0.78	3.4496	0.10
3.6035	0.40	3.5628	0.72	3.4677	0.10
3.6100	0.40	3.5768	0.71	3.5904	0.10
3.7687	0.30	3.7642	0.67	3.6035	0.10
3.7731	0.30	3.7731	0.68	3.7642	0.079
3.8846	0.28	3.8947	0.60	3.7731	0.078
3.8913	0.28	3.9013	0.60	3.8778	0.068
4.0515	0.18	4.0740	0.40	3.8846	0.068
4.0538	0.18	4.0806	0.34	4.0607	0.054
4.1718	0.14	4.2427	0.24	4.0652	0.054
4.1736	0.14	4.2457	0.24	4.2486	0.044
4.3062	0.12	4.3548	0.20	4.2516	0.044
4.2088	0.12	4.3582	0.20	4.4057	0.036
4.4925	0.10	4.4648	0.18	4.4077	0.036
4.4941	0.10	4.4657	0.18	4.5407	0.032
4.6592	0.10	4.5511	0.16	4.5422	0.032
4.6598	0.10	4.5525	0.16	4.6558	0.026
4.7781	0.10	4.6279	0.15	4.6569	0.026
4.7790	0.10	4.6328	0.15	4.8734	0.019
4.8935	0.10	4.8428	0.15	4.8741	0.019
4.8938	0.10	4.8436	0.12	4.9661	0.17

APPENDIX E, CONT.

5° C		25° C		45° C	
B	$Px10^5$	B	$Px10^5$	B	$Px10^5$
5.0157	0.10	4.9316	0.096	4.9667	0.17
5.0163	0.10	4.9322	0.096	5.0648	0.16
5.1663	0.10	4.9981	0.10	5.0652	0.16
5.1667	0.10	4.9991	0.10	5.2032	0.13
5.3410	0.10	5.0589	0.18	5.2035	0.13
5.3412	0.10	5.0598	0.18	5.3920	0.12
5.4645	0.10	5.1066	0.087	5.3922	0.12
5.4646	0.10	5.1075	0.087	5.4743	0.10
5.5375	0.052	5.2053	0.10	5.4743	0.10
5.5376	0.052	5.2087	0.10	5.5404	0.10
5.5377	0.052	5.3013	0.10	5.5405	0.10
		5.3017	0.10	5.5415	0.10
		5.3955	0.10		
		5.3959	0.10		
		5.4686	0.10		
		5.4688	0.10		
		5.5330	0.10		
		5.5331	0.10		
		5.5333	0.10		

APPENDIX F

Pressure-time Histories for TPH 3105 Runs. Preconditioned at 25% R. H. and 75% R. H.

All of these data are from 25° C isotherms. P = bell jar pressure, torr; B = log of the vacuum exposure time in seconds.

25% R.H.		75% R.H.	
B	$Px10^6$	B	$Px10^6$
3.0328	1.4	2.9817	1.4
3.0786	1.2	3.0328	1.4
3.2960	9.0	3.2689	1.0
3.3216	8.8	3.2960	1.0
3.4764	6.4	3.4402	7.2
3.4935	6.6	3.4587	7.0
3.6100	5.5	3.5699	5.9
3.6226	5.5	3.5836	5.8
3.7774	4.4	3.7642	4.6
3.7860	4.4	3.7731	4.6
3.8947	3.6	3.8812	3.8
3.8980	3.6	3.8880	3.8
4.0351	2.8	4.0374	3.0
4.0398	2.8	4.0422	3.0
4.2039	2.1	4.2198	2.3
4.2055	2.1	4.2229	2.3
4.3300	1.8	4.3312	2.0
4.3312	1.8	4.3336	2.0
4.5089	1.4	4.5129	1.6
4.6598	1.2	4.5145	1.6
4.6604	1.2	4.6370	1.4
4.8888	1.0	4.6382	1.4
4.8895	1.0	4.8632	1.1
4.9633	1.0	4.8639	1.1

APPENDIX F, CONT.

25% R.H.	
B	$Px10^6$
4.9639	1.0
5.0190	1.0
5.0195	1.0
5.2114	2.0
5.2119	2.0
5.3970	1.0
5.3971	1.0
5.4768	1.0
5.4770	1.0
5.5375	1.0
5.5376	1.0

75% R.H.	
B	$Px10^6$
4.9867	1.0
4.9873	1.0
5.0804	1.0
5.0808	1.0
5.2092	1.0
5.2095	1.0
5.3319	1.0
5.3321	1.0
5.4527	1.0
5.4529	1.0
5.5375	1.0
5.5377	1.0
5.5378	1.0

APPENDIX G

The Constants for Equation 6

(1) Constants for the Storage Modulus, G'

Temp., ^{o}C	R.H.,%	I	n	Bc
5	50	8.058	0	4.300
25	50	7.857	0.020	4.300
45	50	7.792	0.020	4.300
25	25	7.919	0.0200	4.650
25	75	7.761	0.0200	4.000

(2) Constants for the Loss Modulus, G"

Temp., ^{o}C	R.H.,%	I	n	Bc
5	50	7.317	0	4.400
25	50	6.942	0.025	4.400
45	50	6.638	0.050	4.400
25	25	6.973	0.025	4.400
25	75	6.854	0.025	4.400

APPENDIX H

A Comparison of Storage Moduli Calculated from Equation 6 and the Experimentally Determined Storage Moduli for TPH 3105

The calculated moduli listed below were generated from Equation 6 using the constants of Appendix G. The B=log t column indicates the vacuum exposure of the sample at the test point. The R.H. column indicates the appropriate preconditioning.

Temp., °C	R.H.,%	B=log t	Log G' Calc.	Log G' Exp.
5	50	4.300	8.0581	8.0581
		4.490	8.0751	8.0657
		4.779	8.0985	8.0903
		5.540	8.1460	8.1473
25	50	3.764	7.8735	7.8692
		4.245	7.8824	7.8848
		4.350	7.8897	7.8870
		4.630	7.9185	7.9113
		5.060	7.9589	7.9590
		5.540	7.9968	8.0051
45	50	3.773	7.8079	7.8150
		4.250	7.8174	7.8293
		4.410	7.8307	7.8370
		4.660	7.8567	7.8517
		5.065	7.8944	7.8920
		5.540	7.9317	7.9299
25	75	3.460	7.7705	7.7663
		3.770	7.7768	7.7871
		4.220	7.7876	7.8154
		4.330	7.8001	7.8298
		5.080	7.8884	7.9042
		5.540	7.9228	7.9619
25	25	3.777	7.9347	7.9332
		4.205	7.9433	7.9392
		4.65	7.9524	7.9619
		4.889	7.9768	7.9683
		5.211	8.0062	7.9961
		5.54	8.0342	8.0269

APPENDIX I

A Comparison of Loss Moduli Calculated from Equation 6 and the Experimentally Determined Loss Moduli for TPH 3105

The calculated moduli listed below were generated from Equation 6 using the constants of Appendix G. The B=log t column indicates the vacuum exposure of the sample at the test point. The R.H. column indicates the appropriate preconditioning.

Temp., °C	R.H., %	B=log t	Log G' Calc.	Log G' Exp.
5	50	4.300	7.3172	7.3201
		4.490	7.3253	7.3253
		4.779	7.3506	7.3506
		5.016	7.3668	7.3759
		5.540	7.3993	7.4208
25	50	3.773	6.9615	6.9318
		4.358	6.9761	7.9778
		4.465	6.9842	6.9926
		4.630	7.0038	7.0043
		5.060	7.0424	7.0610
		5.540	7.0878	7.1244
45	50	3.773	6.6766	6.6572
		4.400	6.7083	6.6989
		4.540	6.7273	6.7231
		4.656	6.7433	6.7233
		5.200	6.8088	6.8051
		5.540	6.8471	6.8446
25	75	3.773	6.8731	6.8604
		4.331	6.8872	6.9009
		4.512	6.8998	6.9197
		4.860	6.9385	6.9467
		5.210	6.9717	6.9800
		5.540	6.9994	7.0224
25	25	3.777	6.9919	6.9907
		4.33	7.0058	6.9974
		4.51	7.0184	7.0294
		4.89	7.0602	7.0469
		5.02	7.0728	7.0641
		5.54	7.1181	7.1324

REFERENCES

1. Greenwood, L. R.: The Effect of Vacuum on the Mechanical Properties of a Solid Rocket Propellant During Space Storage. Ph.D. Thesis, Virginia Polytechnic Institute, 1967.

2. Mugler, J. P. Jr.; Greenwood, L. R.; Lassiter, W. S.; and Comparin, R. A.: In Situ Vacuum Testing - A Must for Certain Elastomeric Materials. J. Spacecraft and Rockets, vol. 6, no. 2, Feb. 1969, pp. 219-221.

3. Greenwood, L. R.; and Ward, T. C.: Prediction of Long-Term Vacuum Effects on Mechanical Properties of a Heat Shield Material. Proc. Institute Environmental Sciences, April, 1971 pp. 435-439.

4. Strauss, E. L.: Superlight Ablative Systems for Mars Lander Thermal Protection. J. Spacecraft and Rockets, vol. 4, no. 10, 1967, pp. 1304-1309.

5. Landel, R. F.; and Moser, B. G.: The Effects of Moisture on the Dynamic Mechanical Properties of Ammonium Perchlorate - Polyurethane Propellants. JPL-TR-32-389 (contract NAS 7-100), 1963.

6. Colodny, P. C.; and Ketchum, G. F.: Humidity and Temperature Effects on the Creep Behavior of Solid Propellants. Bullitin of 4th Meeting of the Interagency Chemical Rocket Propulsion Group, Oct., 1965, pp. 135-139.

7. Oberth, A. E.; and Bruenner, R. S.: The Cause of Moisture Embrittlement in Solid Propellants. Presented to theInteragency Chemical Rocket Propulsion Group, 1966, AFSC-66-951.

8. McCrum, N. G.; Read, B. E.; and Williams, G.: Anelastic and Dielectric Effects in Polymeric Solids. John Wiley and Sons, Inc., 1967.

9. Ward, T. C.; and Tobolsky, A. V.: A Viscoelastic Study of Ionomers. J. Appl. Polym. Sci., vol. 11, p. 2403, 1967.

10. Tobolsky, A. V.: Properties and Structure of Polymers. John Wiley and Sons, Inc., 1960.

11. Ferry, J. D.: Viscoelastic Properties of Polymers. Second ed., John Wiley and Sons, Inc., 1970.

12. Williams, M. L.; Landel, R. F.; and Ferry J. D.: The Temperature Dependence of Relaxation Mechanisms in Amorphous Polymers and other Glass-forming Liquids. J. Amer. Chem. Soc., vol. 77, pp 3701-3707, 1955.

13. Smith, T. L.: Strength and Extensibility of Elastomers. Chapter 4 of Rheology, vol. 5, ed. by Eirich, F. R.. Academic Press, Inc., 1969.

14. Payne, A. R.: Physics and Physical Testing of Polymers. Chapter 1 of Progress in High Polymers, vol. 5, ed. by Robb, J. C.; and Peaker, F. W.. CRC Press, Inc., Cleveland, 1968.

15. Martin, D. L.: The Effect of Filler Concentration on the Viscoelastic Response of a Composite Solid Propellant. RK-TR-64-2 (AD-433612), 1964.

16. Schwarzl, F. R.: On Mechanical Properties of Unfilled and Filled Elastomers. From the Mechanics and Chemistry of Solid Propellants, ed. by Eringen, A. C.; Liebowitz, H.; Koh, S. L.; and Crowley, J. M.; Pergamon Press, pp. 503-539, 1965.

17. Quistwater, J. M. R.; and Dunell, B. A.: Dynamic Mechanical Properties of Nylon 66 and the Plasticizing Effect of Water Vapor on Nylon. J. of Appl. Polymer Sci., vol. 1, pp 267-271, 1959.

18. Nielsen, L. E.: A recording Torsion Pendulum for the Measurement of the Dynamical Mechanical Properties of Plastics and Polymers. Review of Scientific Instruments, vol. 33, no. 9, Sept., 1951.

19. Hay, T.: Summary of Martin Marietta Co. Material Properties. A Review presented at Mini-Symposium on the Environmental Testing of SLA 561 Heat Shield Material, NASA Langley Research Center, Oct. 20, 1970.

20. Private communication with the General Electric Co., 1970.

21. American Society for Testing Materials: Maintaining Constant Relative Humidity by Means of Aqueous Solutions. ASTM E 104-51.

REFERENCES, CONT.

22. Zappas, L. Private communication relaying data of test run at the National Bureau of Standards, July 22, 1971.

23. Platzer, N. A. J.: Plasticization and Plasticizer Processes. Advances in Chemistry Series, vol 48, The American Chemical Society, Washington, 1965.

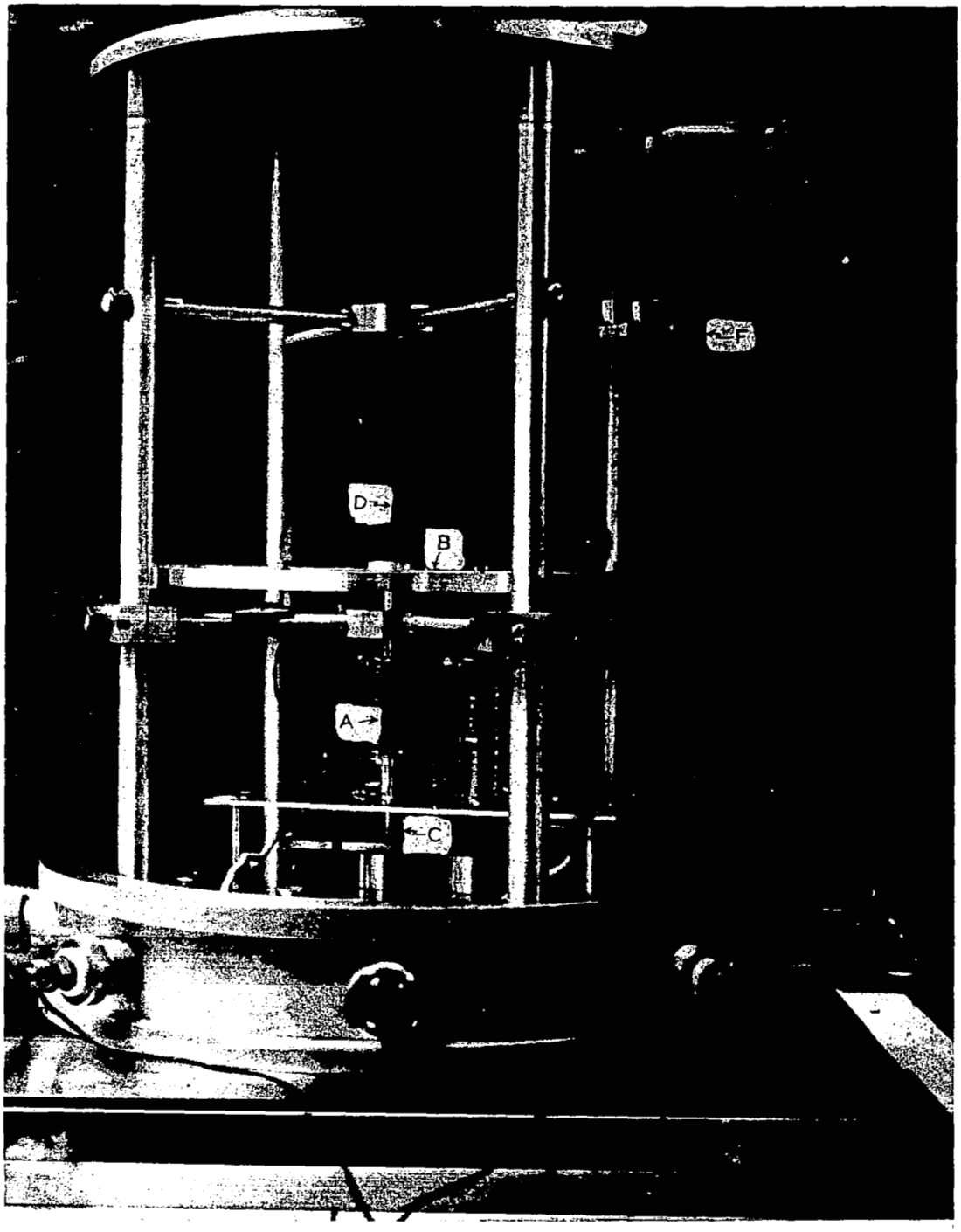

Figure 1. The Torsion Pendulum.

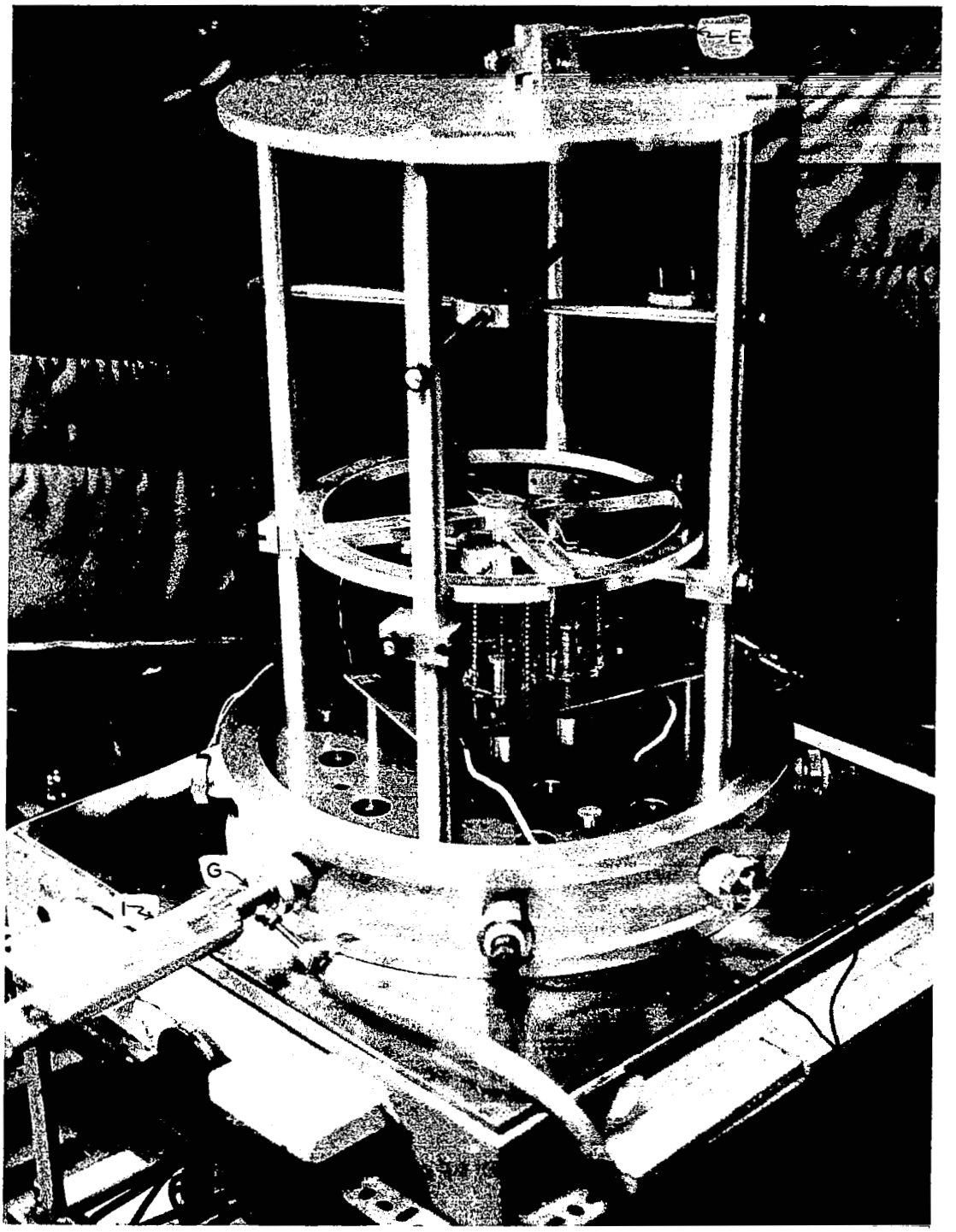

Figure 2. The Torsion Pendulum, Top-Front View.

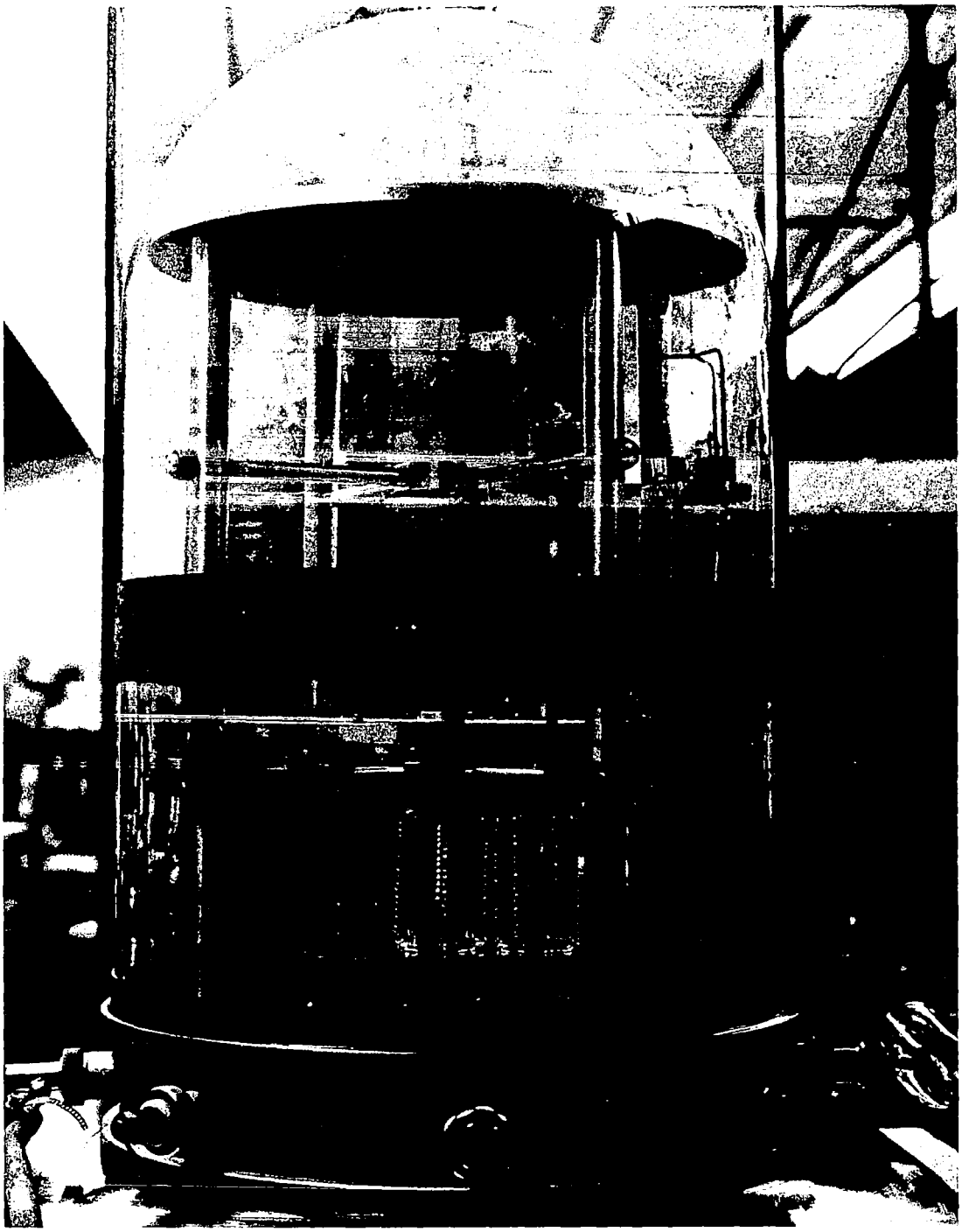

Figure 3. The Torsion Pendulum with the Bell Jar in Place.

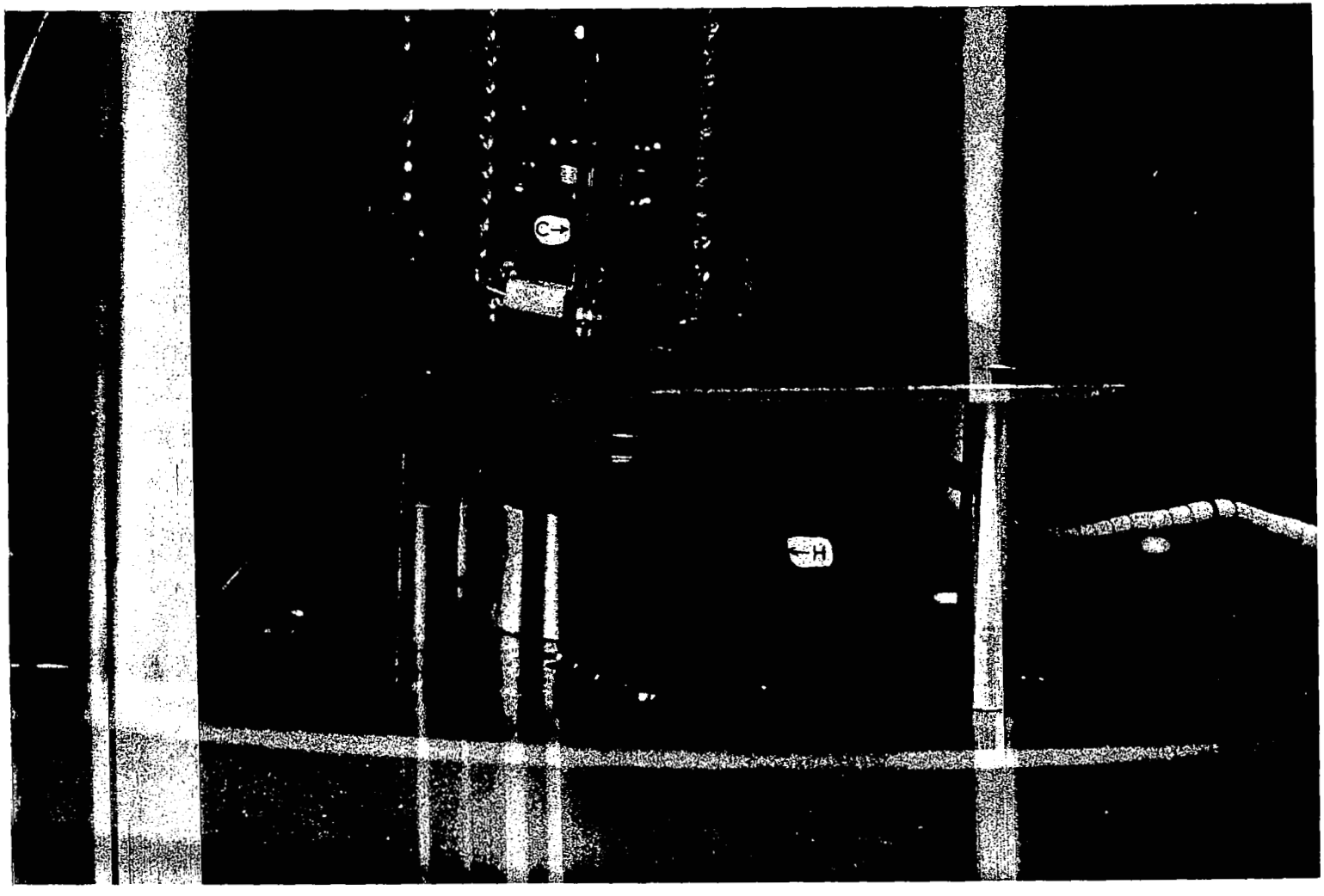

Figure 4. Detail of the Torsion Pendulum Activation Mechanism.

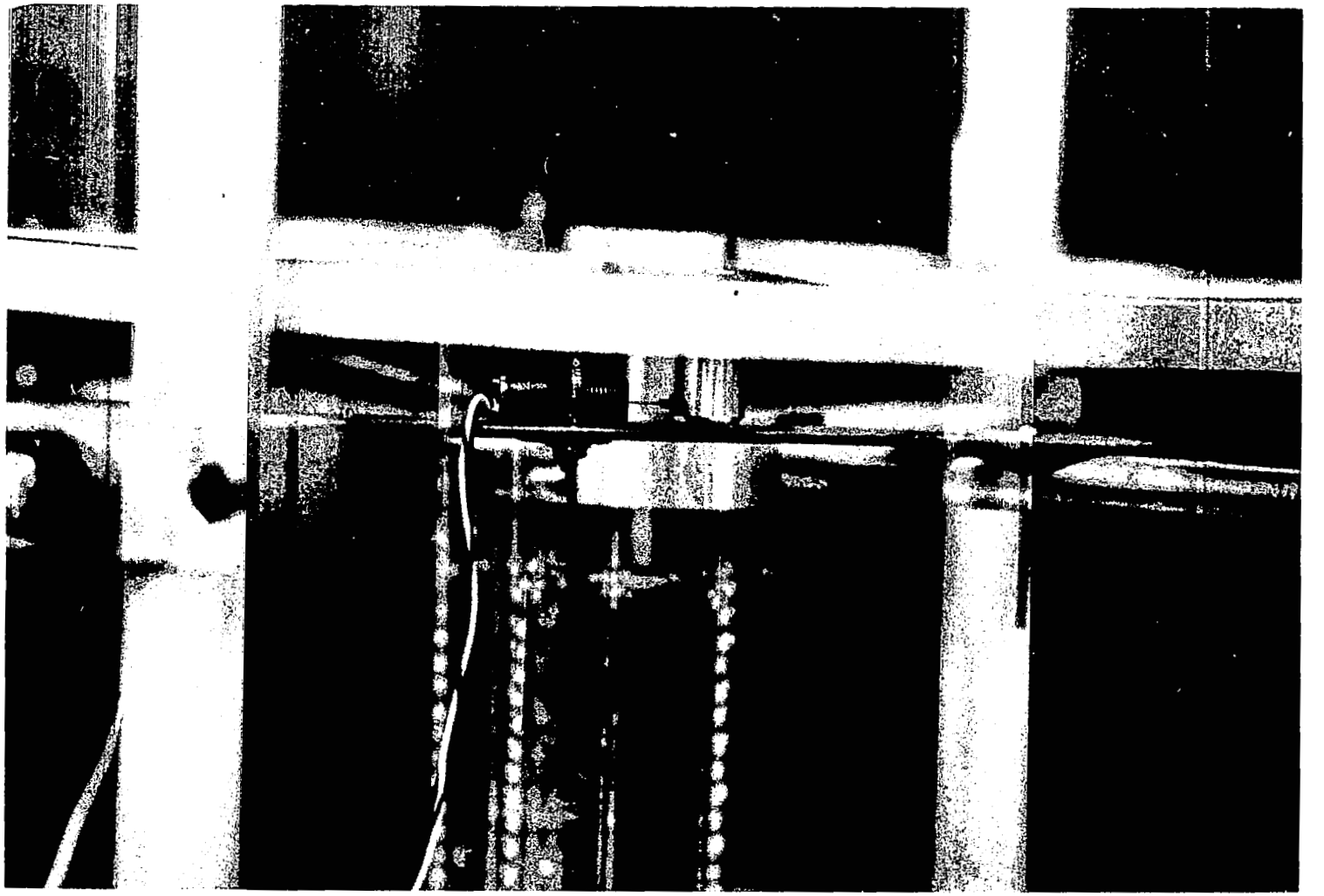

Figure 5. Detail of the Torsion Pendulum Showing the LVDT.

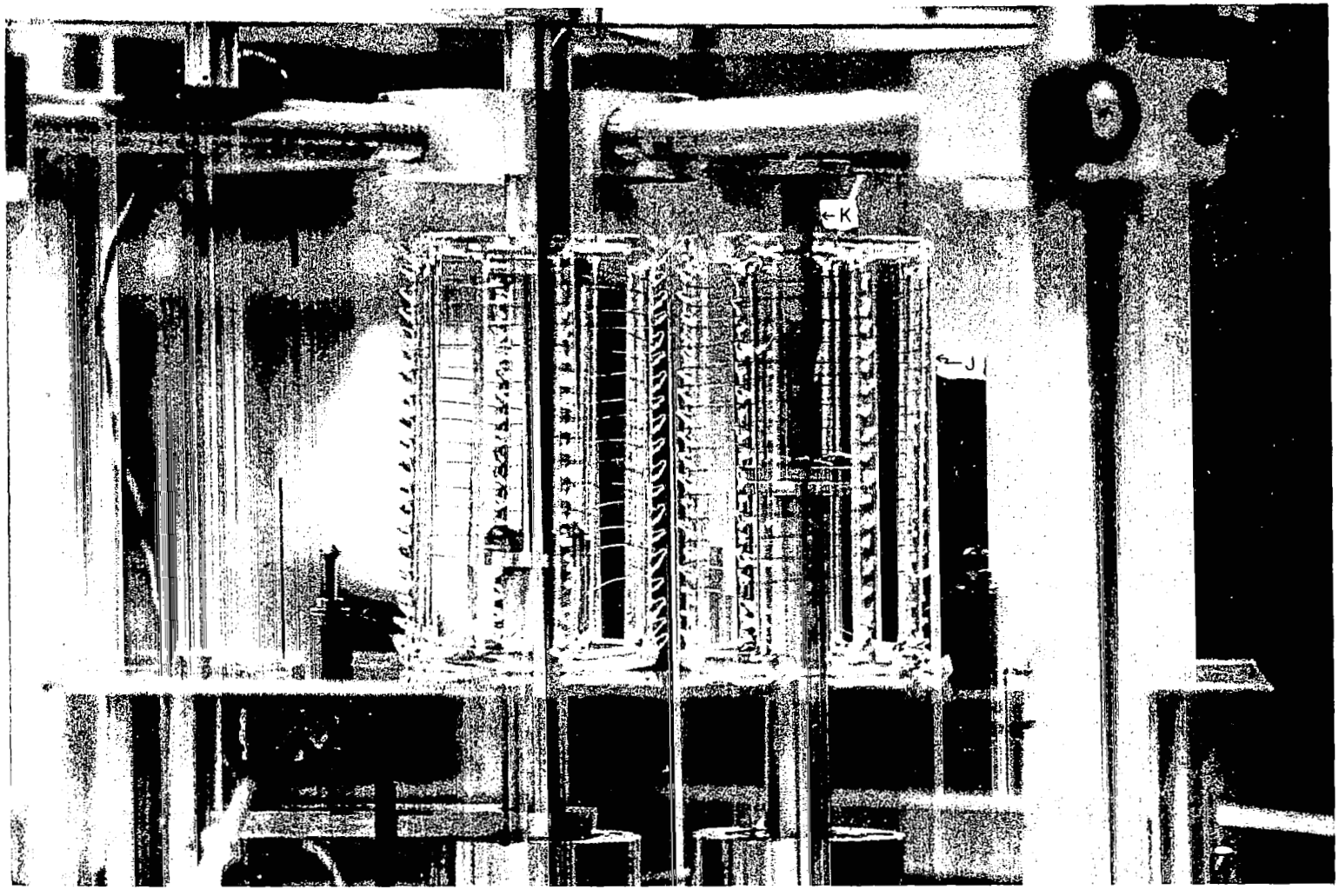

Figure 6. Detail of the Torsion Pendulum Heating Coils.

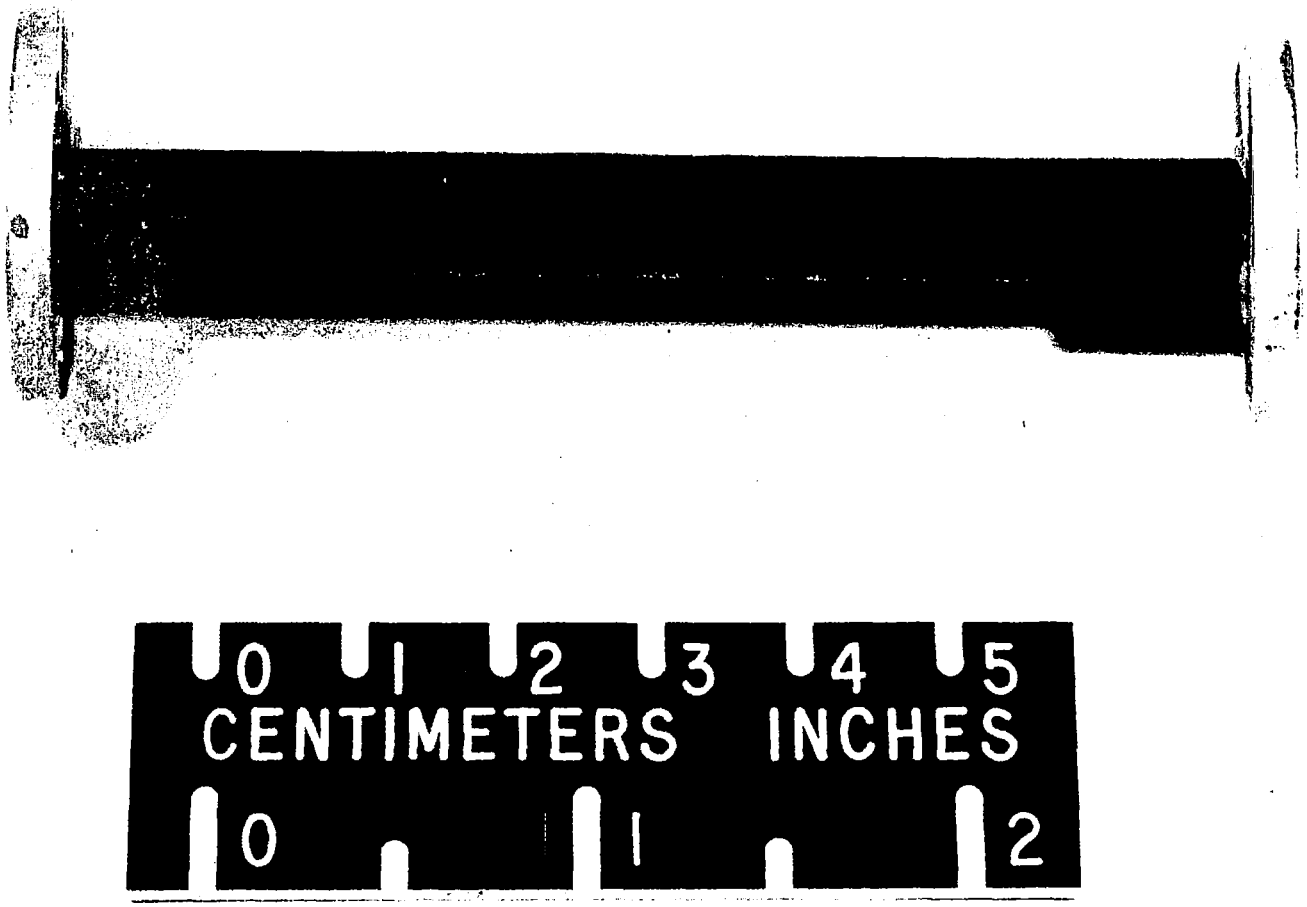

Figure 7. A Sample Prepared for Testing.

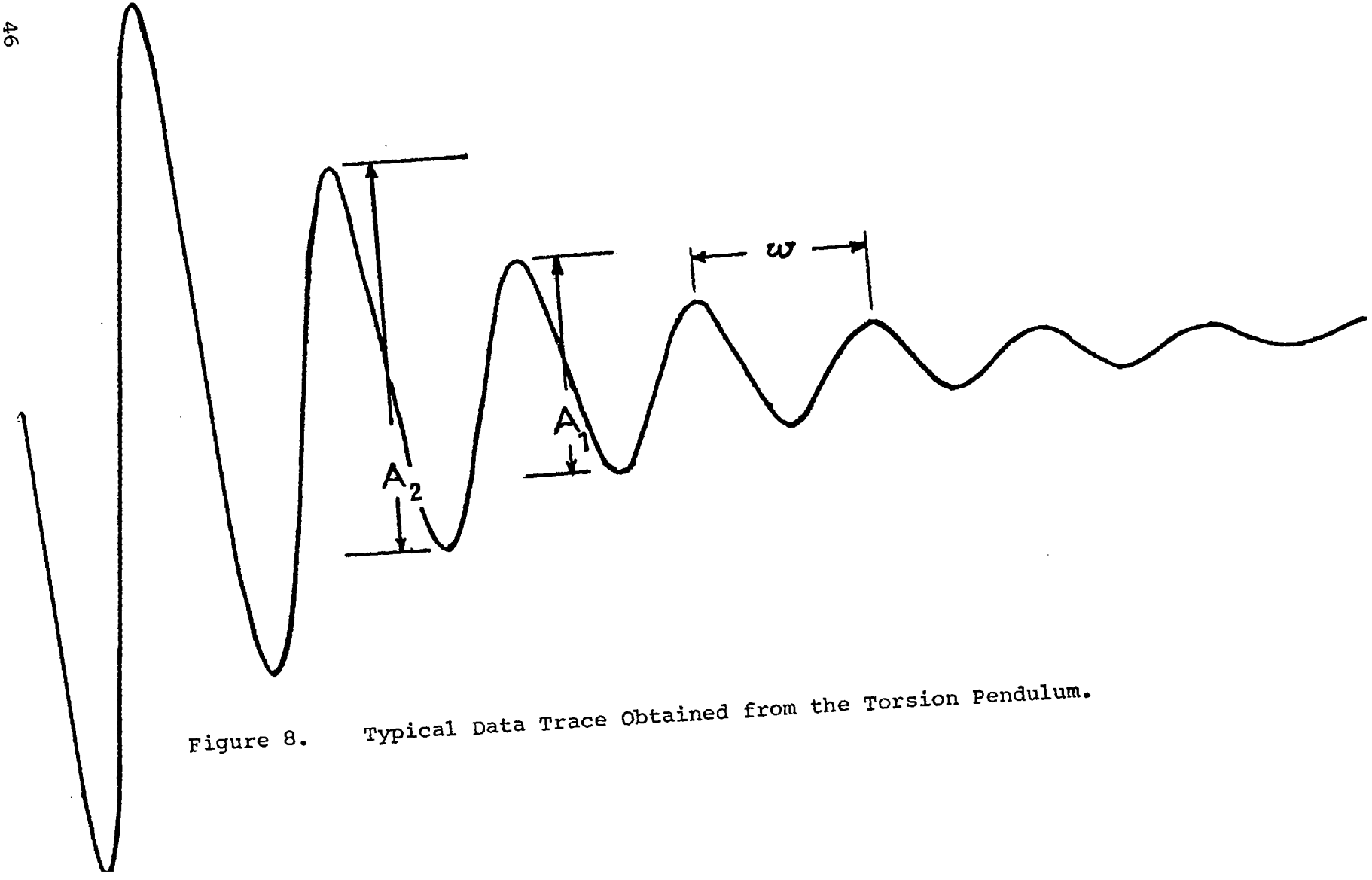

Figure 8. Typical Data Trace Obtained from the Torsion Pendulum.

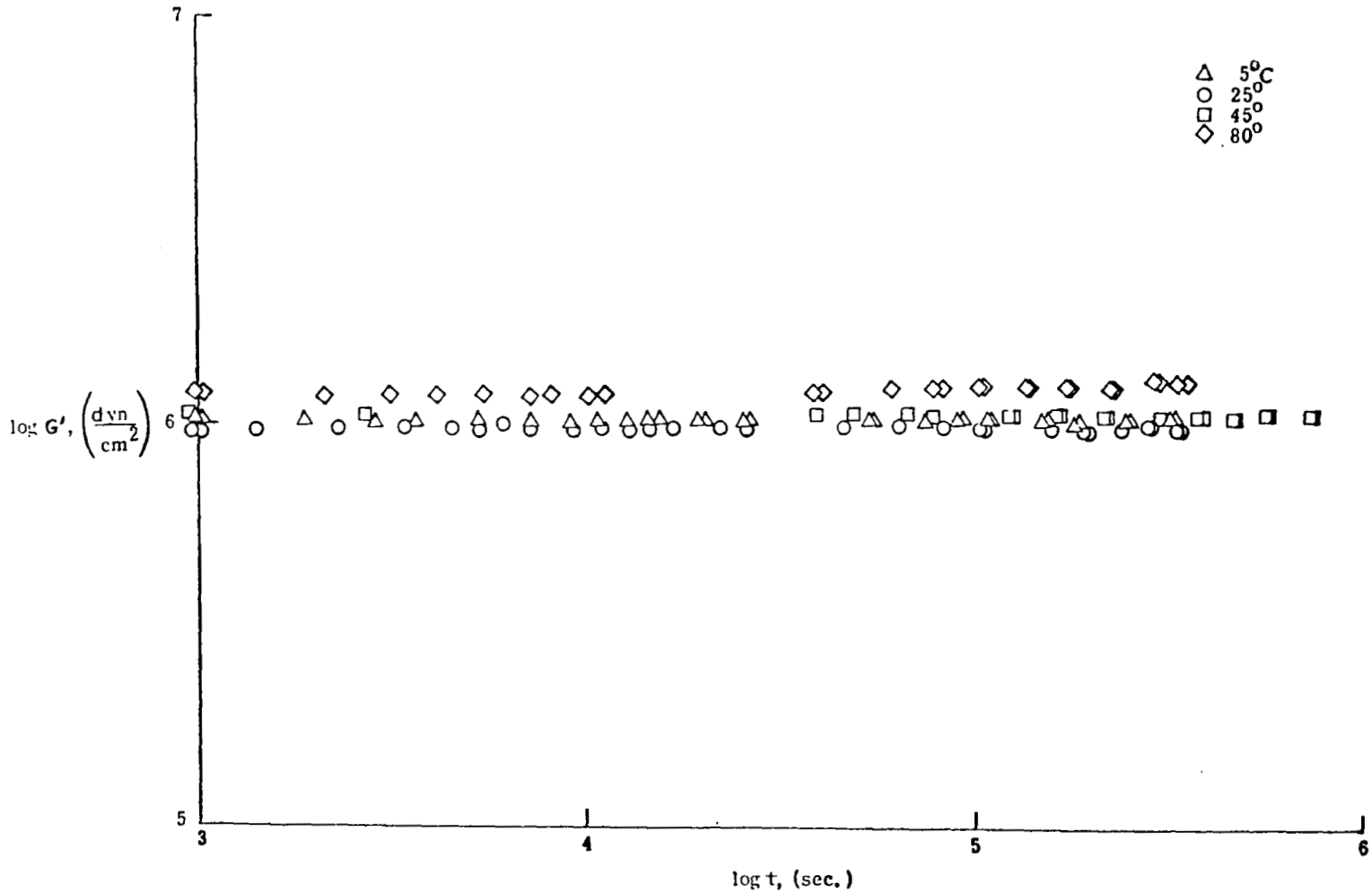

Figure 9. The Influence of Vacuum Exposure on the Storage Modulus of ESM 1004x at Four Temperatures.

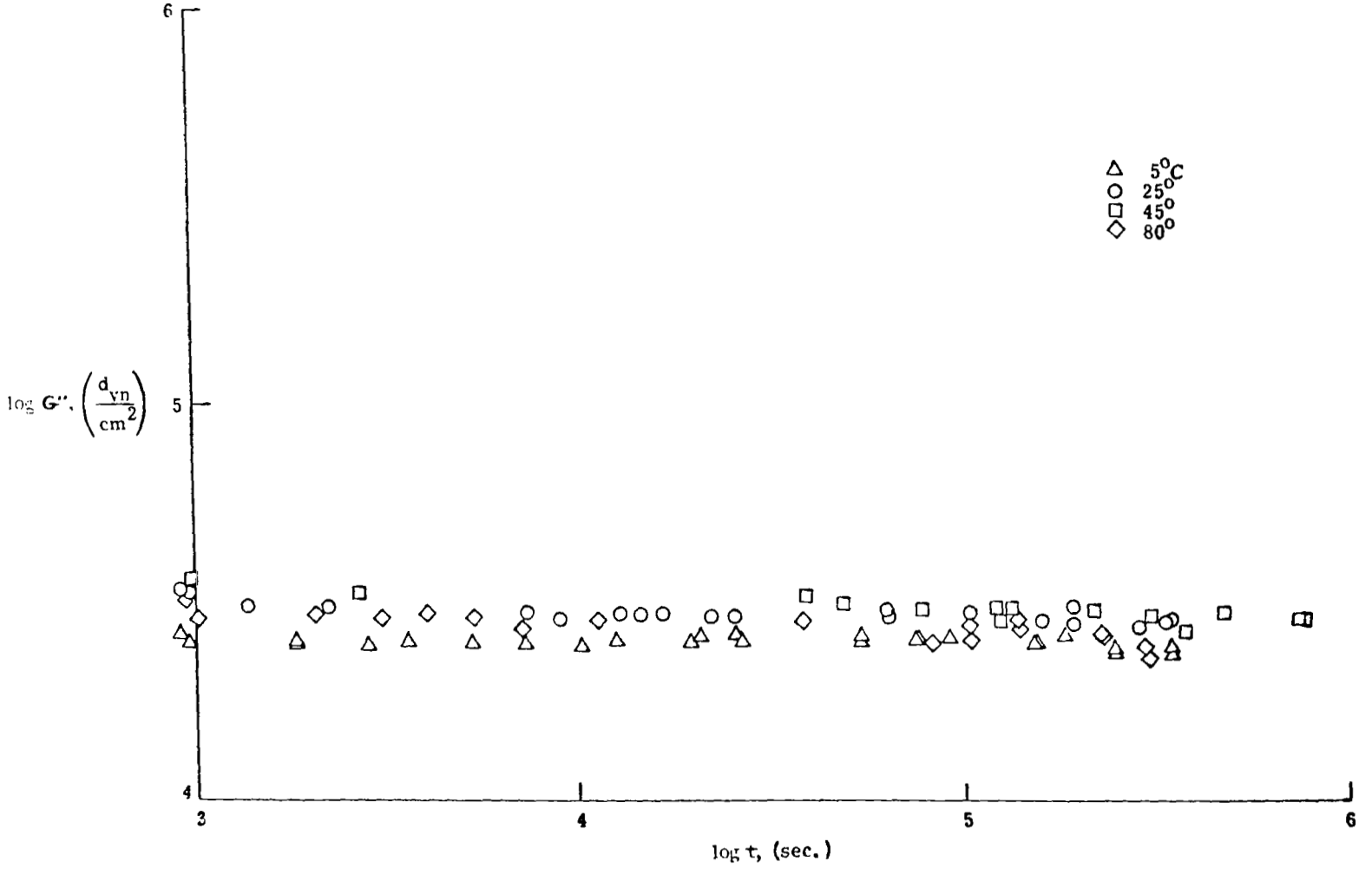

Figure 10. The Influence of Vacuum Exposure on the Loss Modulus of ESM 1004x at Four Temperatures.

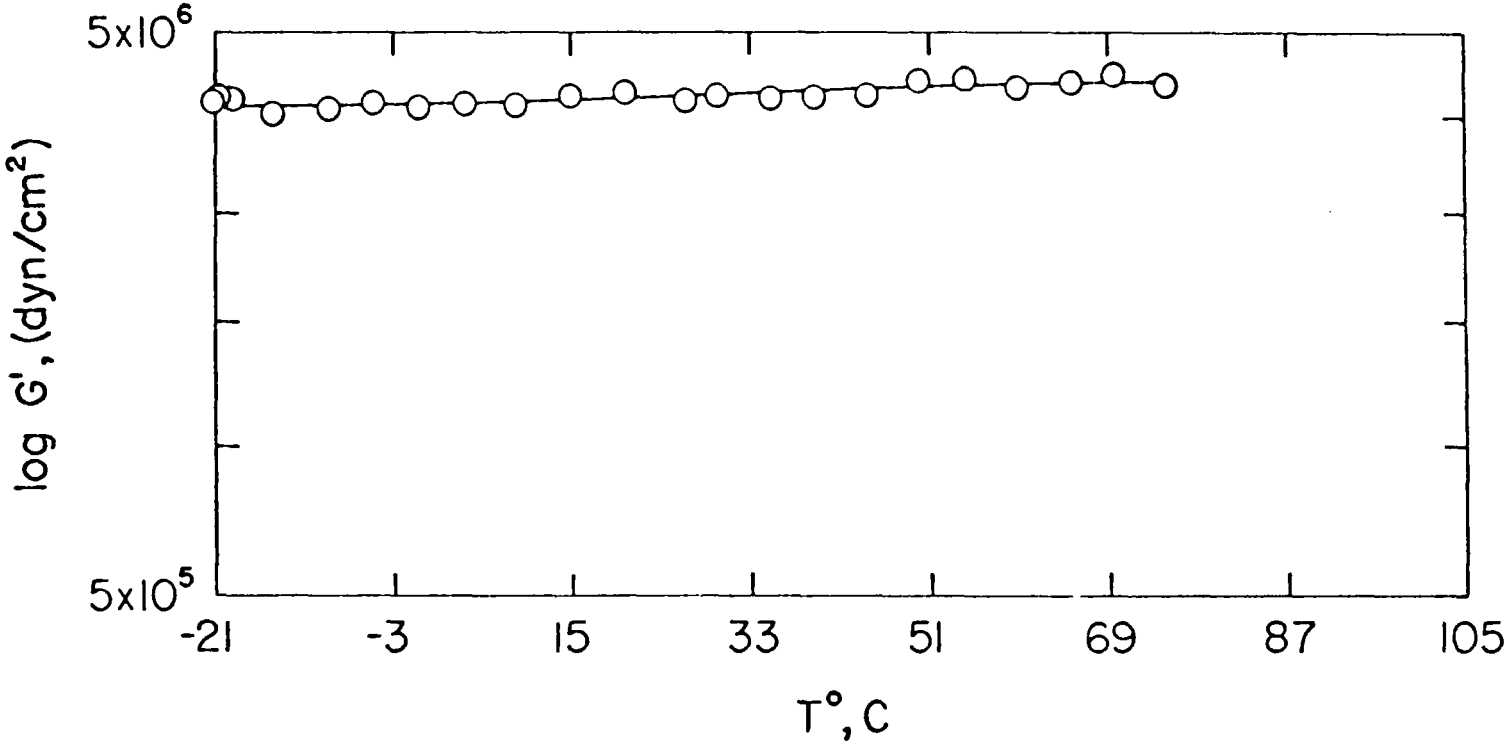

Figure 11. Variation of the ESM 1004x Storage Modulus with Temperature. Sample preconditioned at 50% R.H.. All points from data at atmospheric pressure.

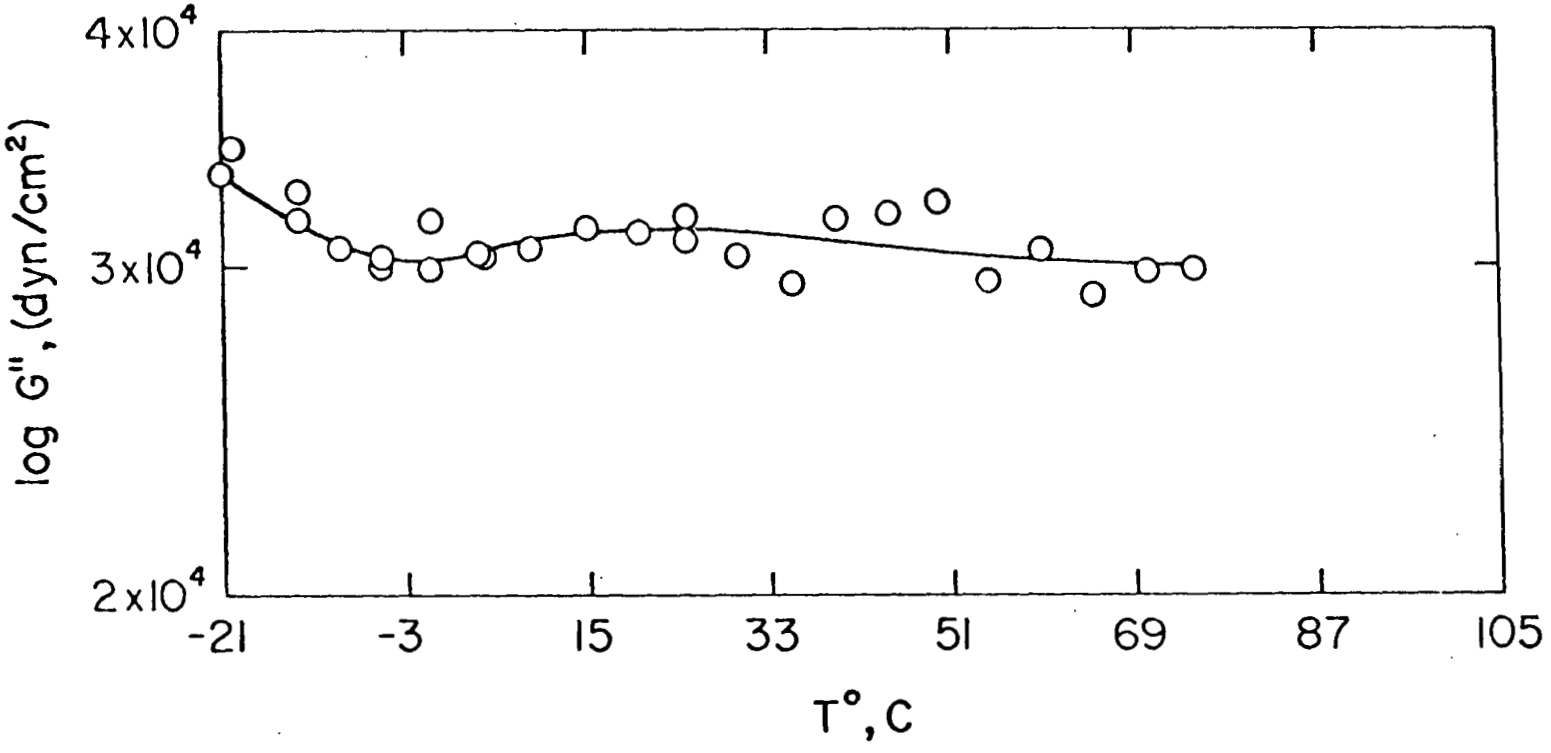

Figure 12. Variation of the ESM 1004x Loss Modulus with Temperature. Sample preconditioned at 50% R.H.. All points from data taken at atmospheric pressure.

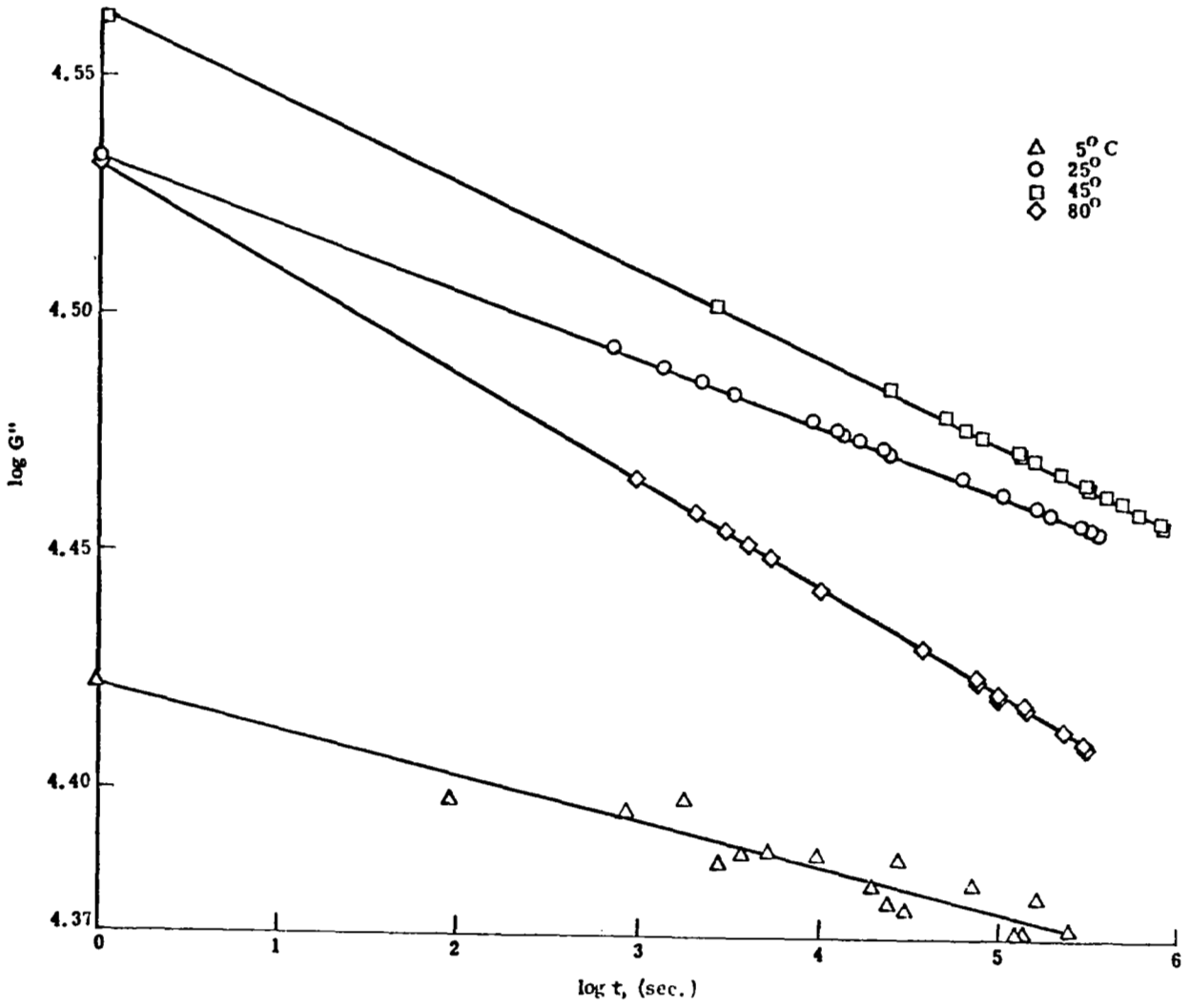

Figure 13. Expanded Scale Plot of ESM 1004x Loss Modulus Isotherms as Functions of Vacuum Exposure. Points at 5° C are actual data, other points are predicted from least squares regression analysis.

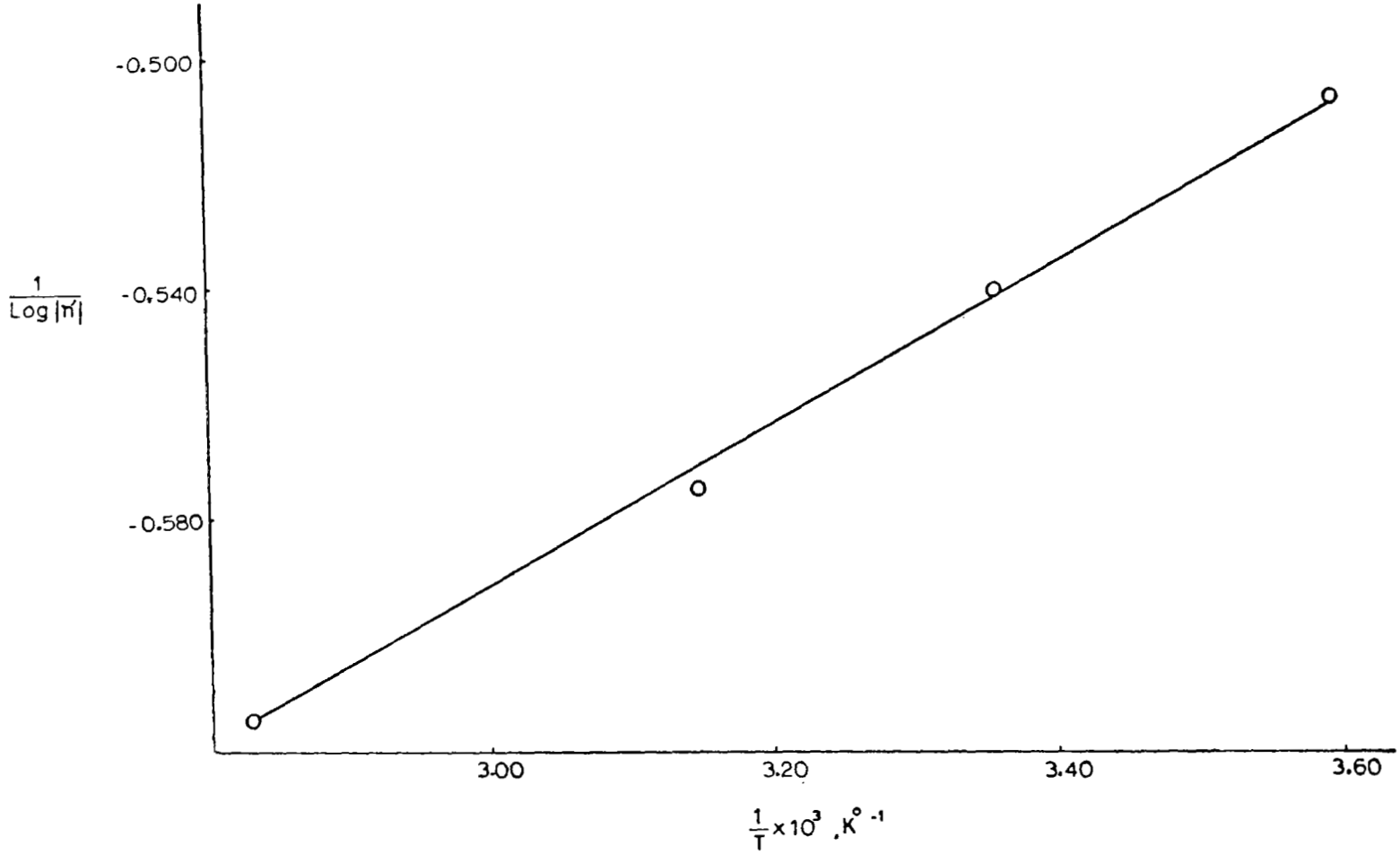

Figure 14. Influence of Temperature on the Rate of ESM 1004x Loss Modulus Decrease. |n'| is absolute value of slope of lines of Figure 13.

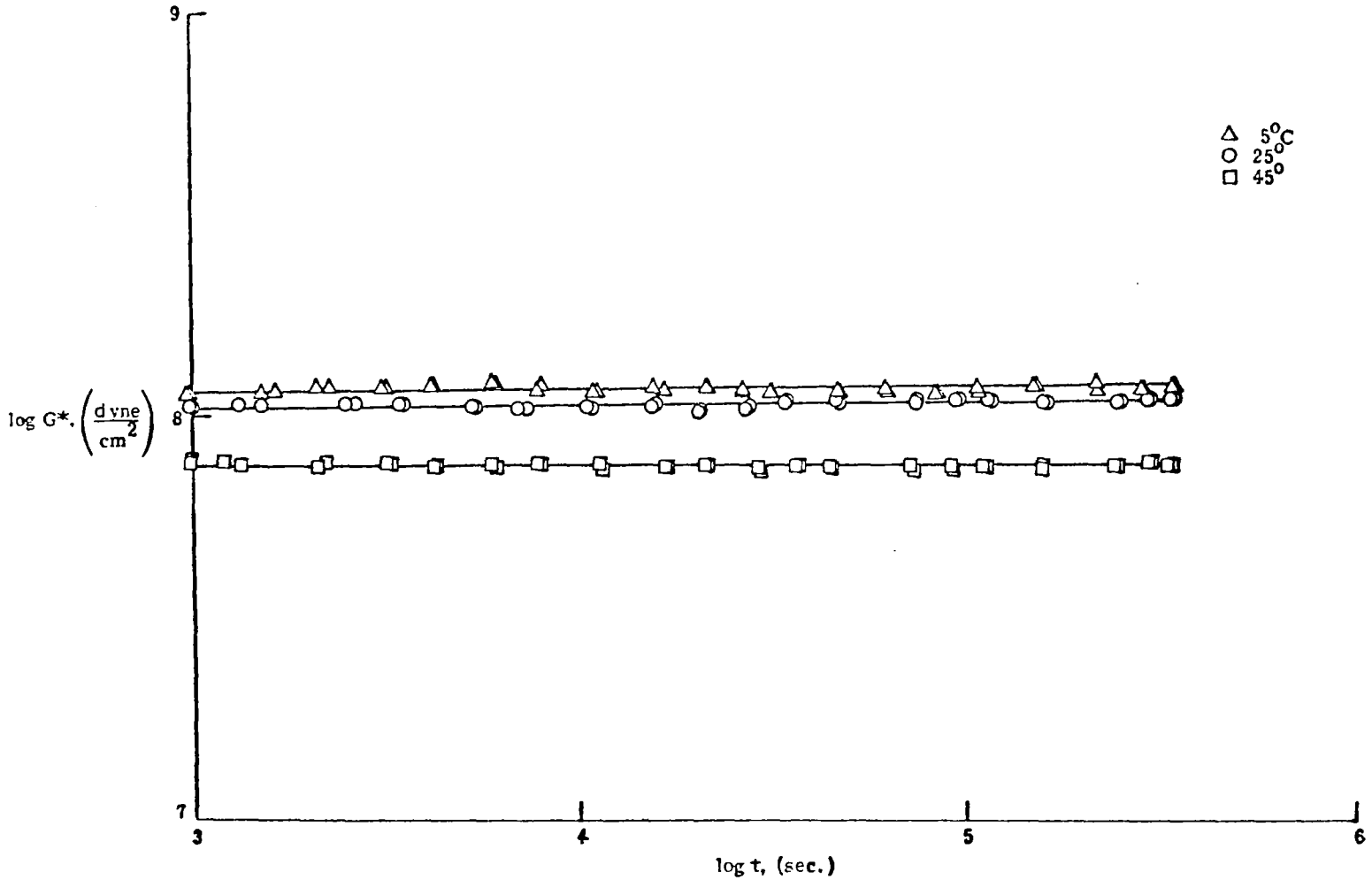

Figure 15. Vacuum Environment Effects on the Complex Modulus of SLA 561v at Three Temperatures. Samples preconditioned at 50% R.H..

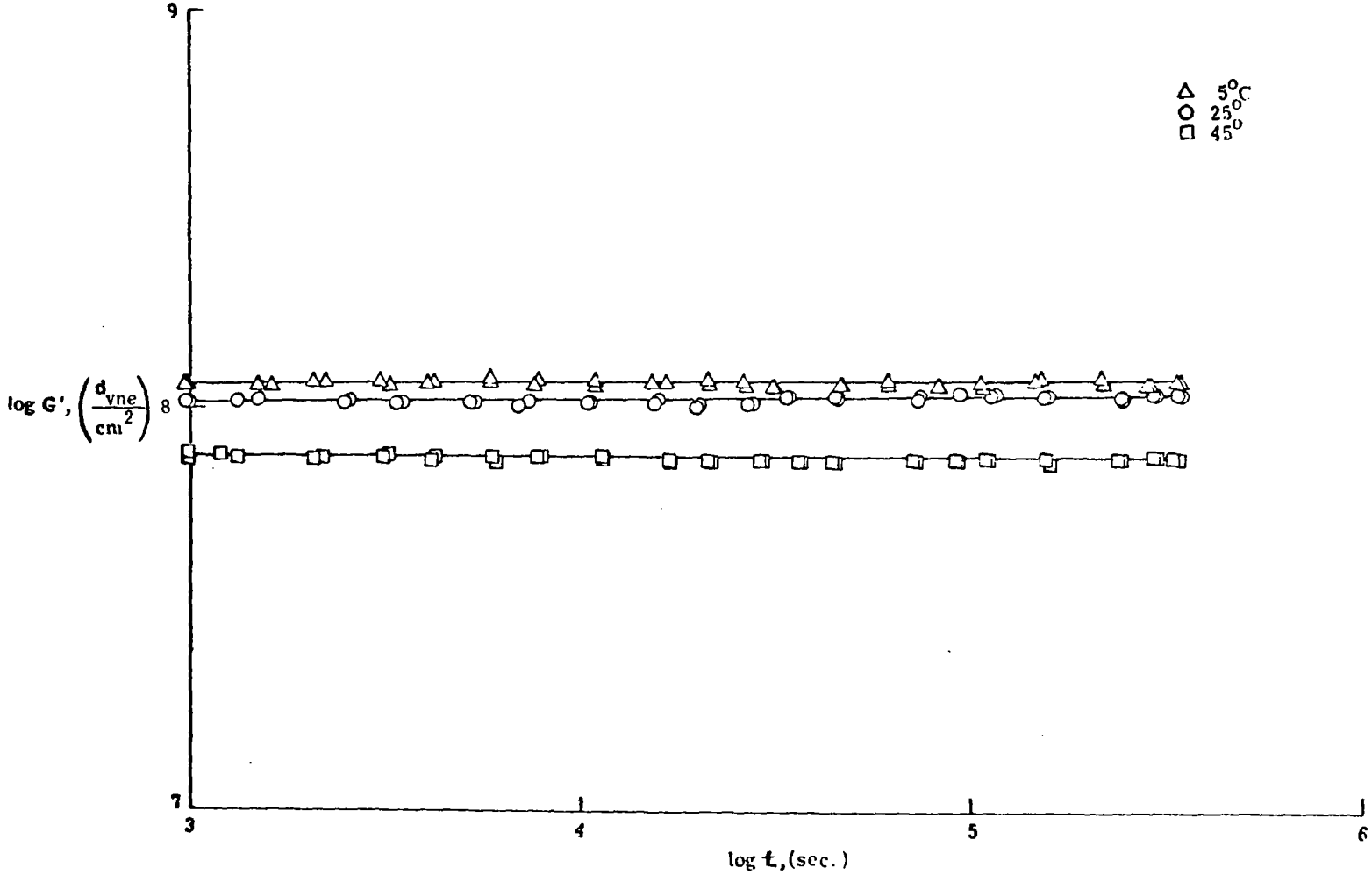

Figure 16. Vacuum Exposure Effects on the Storage Modulus of SLA 561v at Three Temperatures. Samples preconditioned at 50% R.H..

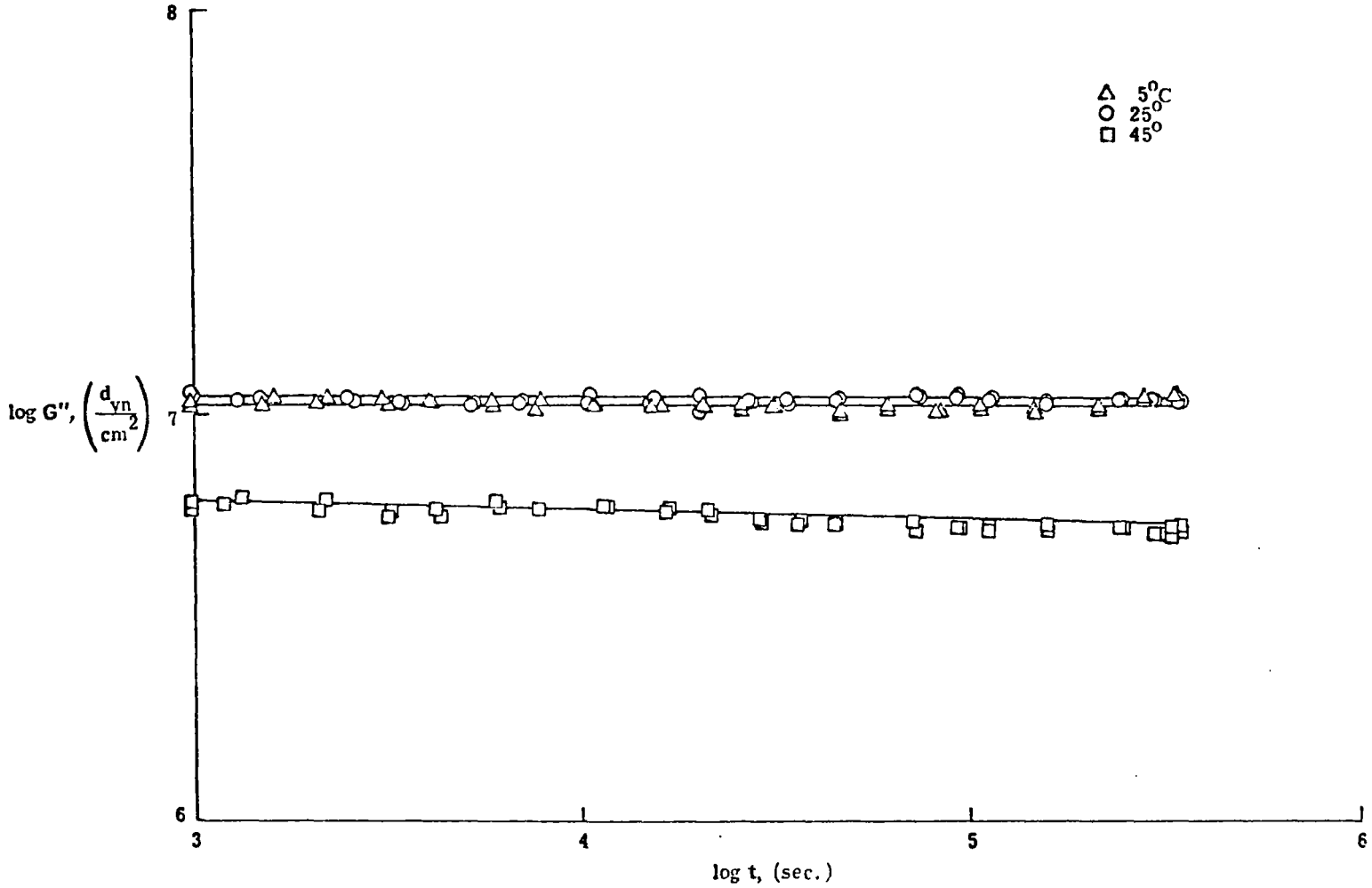

Figure 17. Vacuum Exposure Effects on the Loss Modulus of SLA 561v at Three Temperatures. Samples preconditioned at 50% R.H..

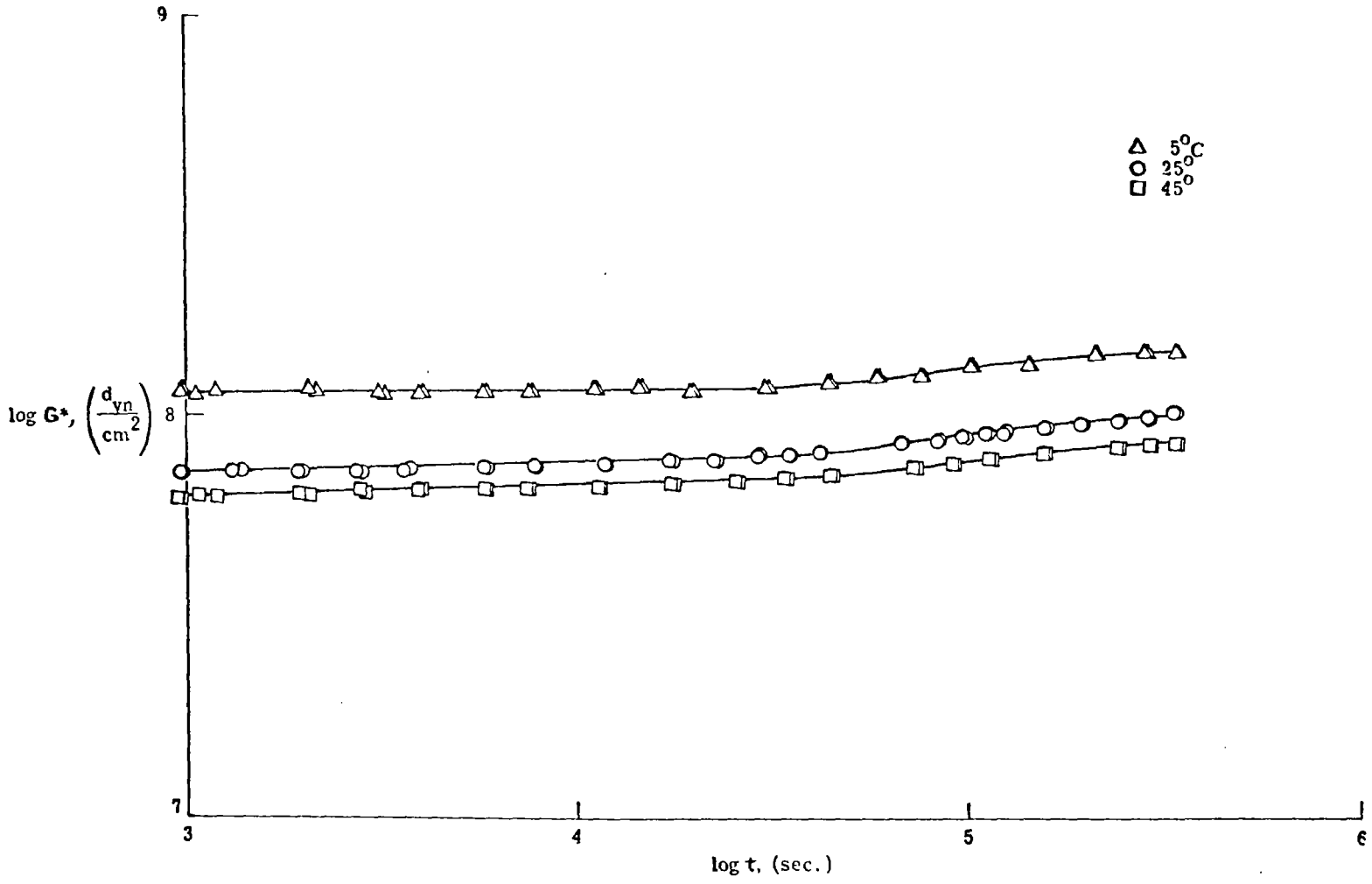

Figure 18. Vacuum Exposure Effects on the Complex Modulus of TPH 3105 at Three Temperatures. Samples preconditioned at 50% R.H..

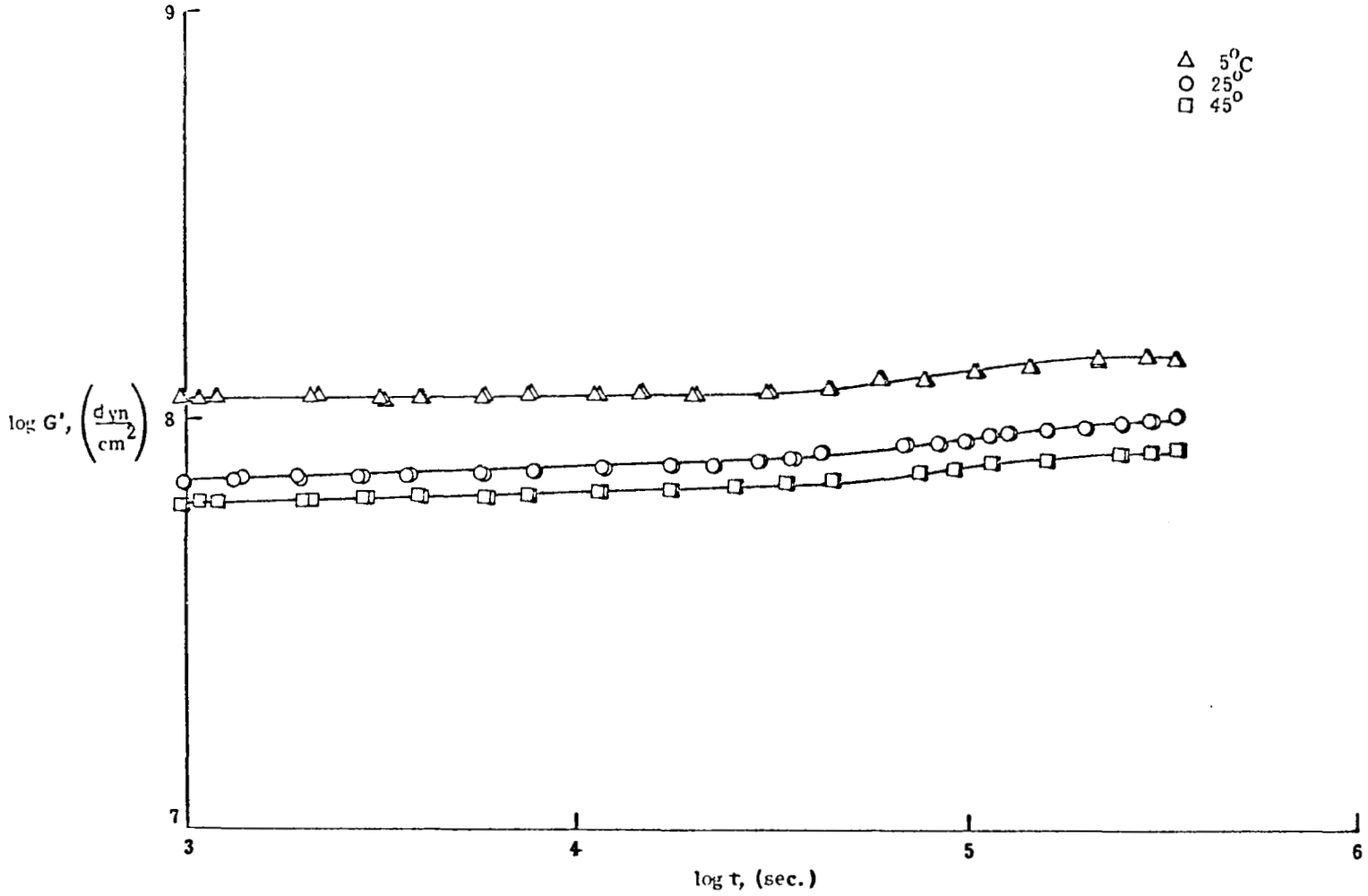

Figure 19. Vacuum Exposure Effects on the Storage Modulus of TPH 3105 at Three Temperatures. Samples preconditioned at 50% R.H..

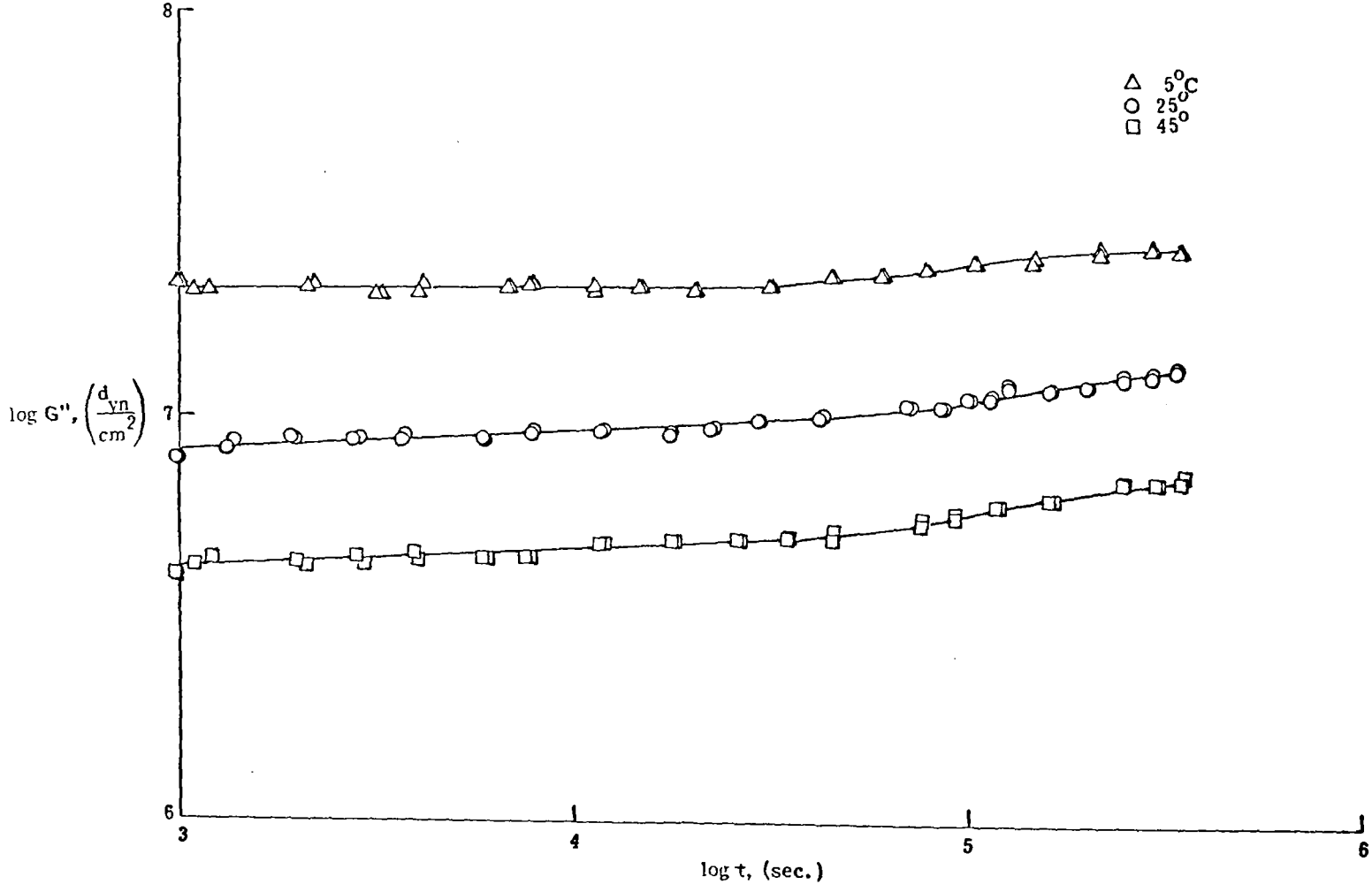

Figure 20. Vacuum Exposure Effects on the Loss Modulus of TPH 3105 at Three Temperatures. Samples preconditioned at 50% R.H..

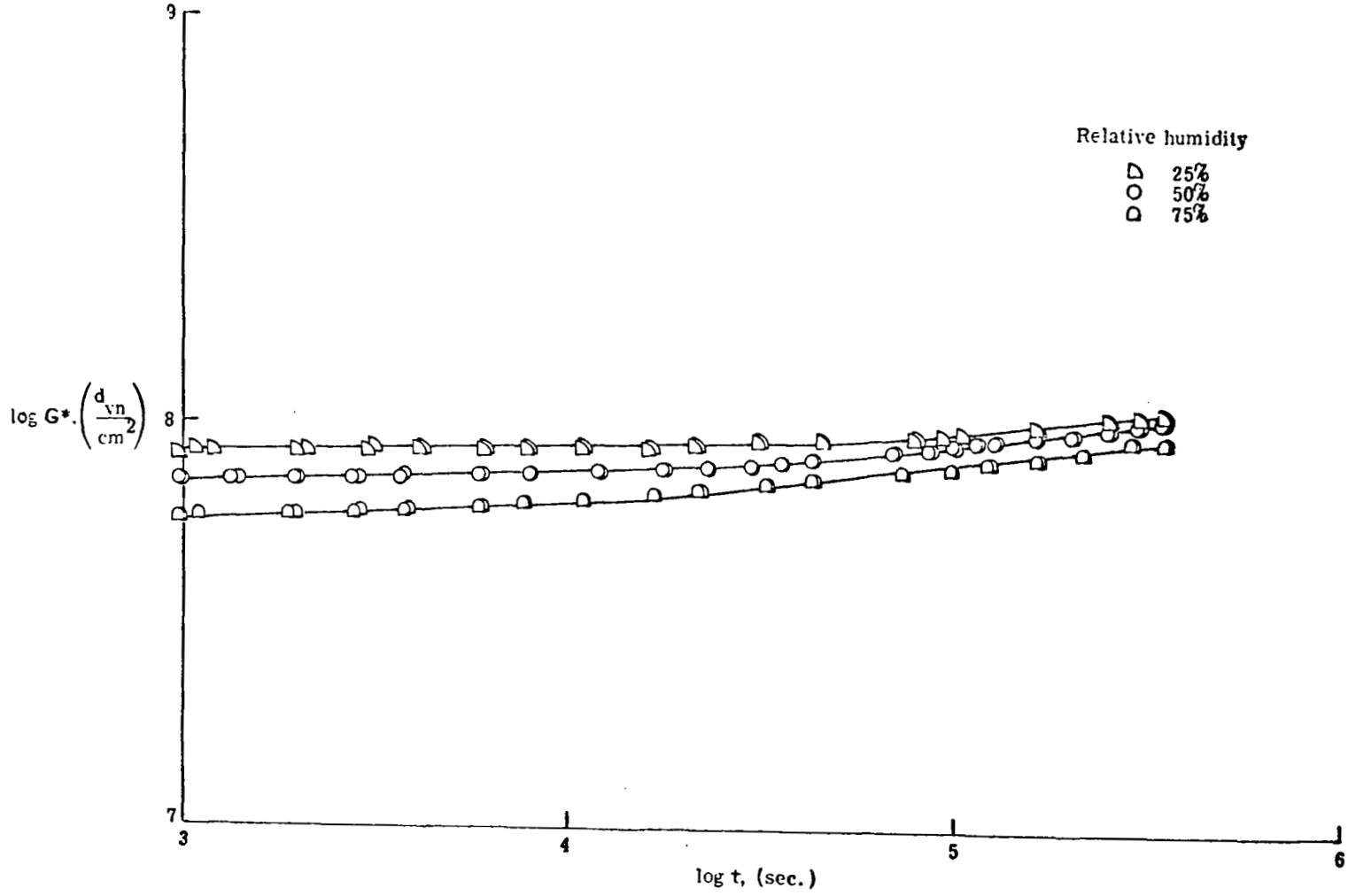

Figure 21. Preconditioning Differences Reflected in the Complex Modulus of TPH 3105 during Vacuum Exposure. All samples run at 25° C.

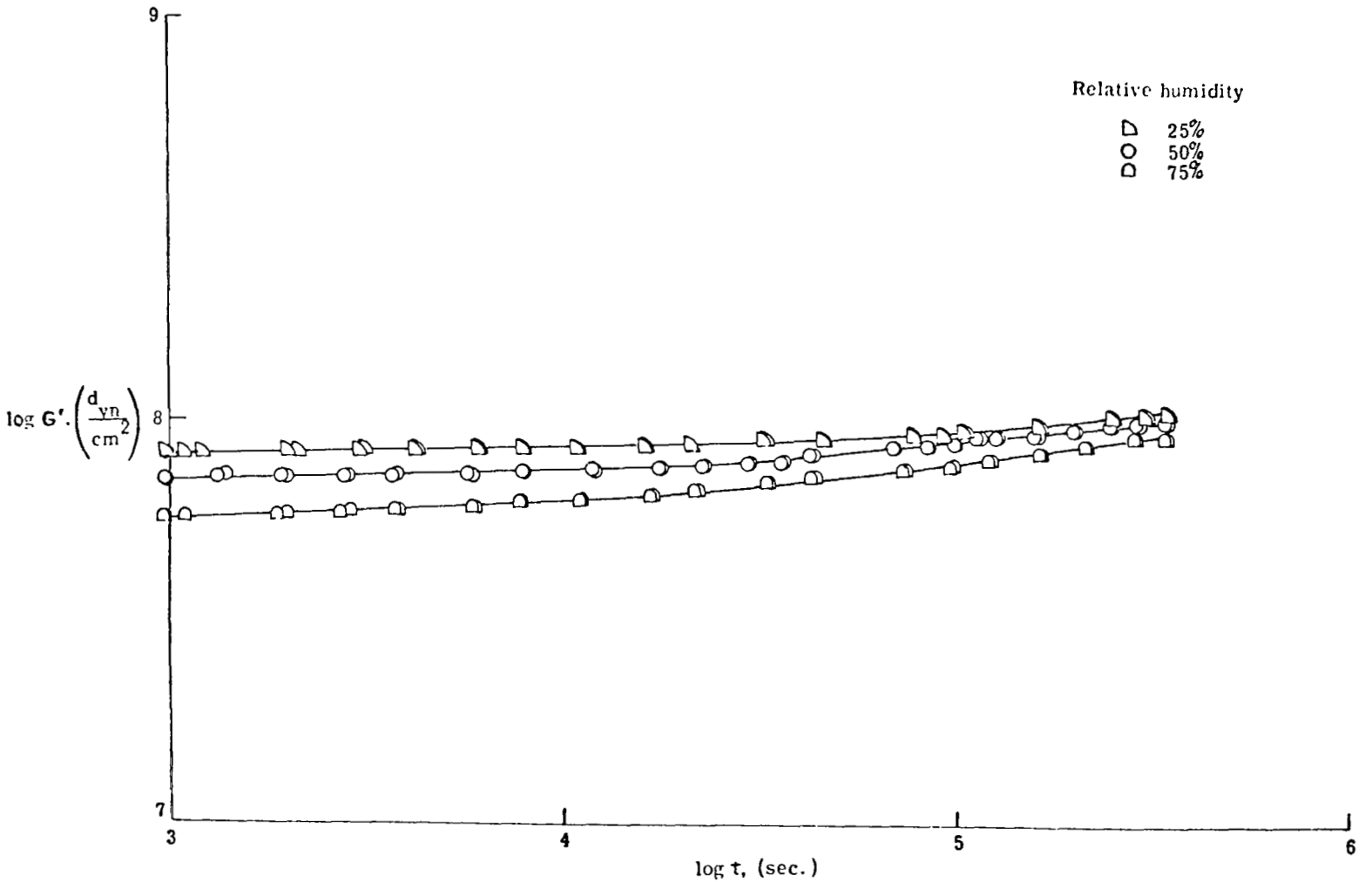

Figure 22. Preconditioning Differences Reflected in the Storage Modulus of TPH 3105 during Vacuum Exposure. All samples run at 25° C.

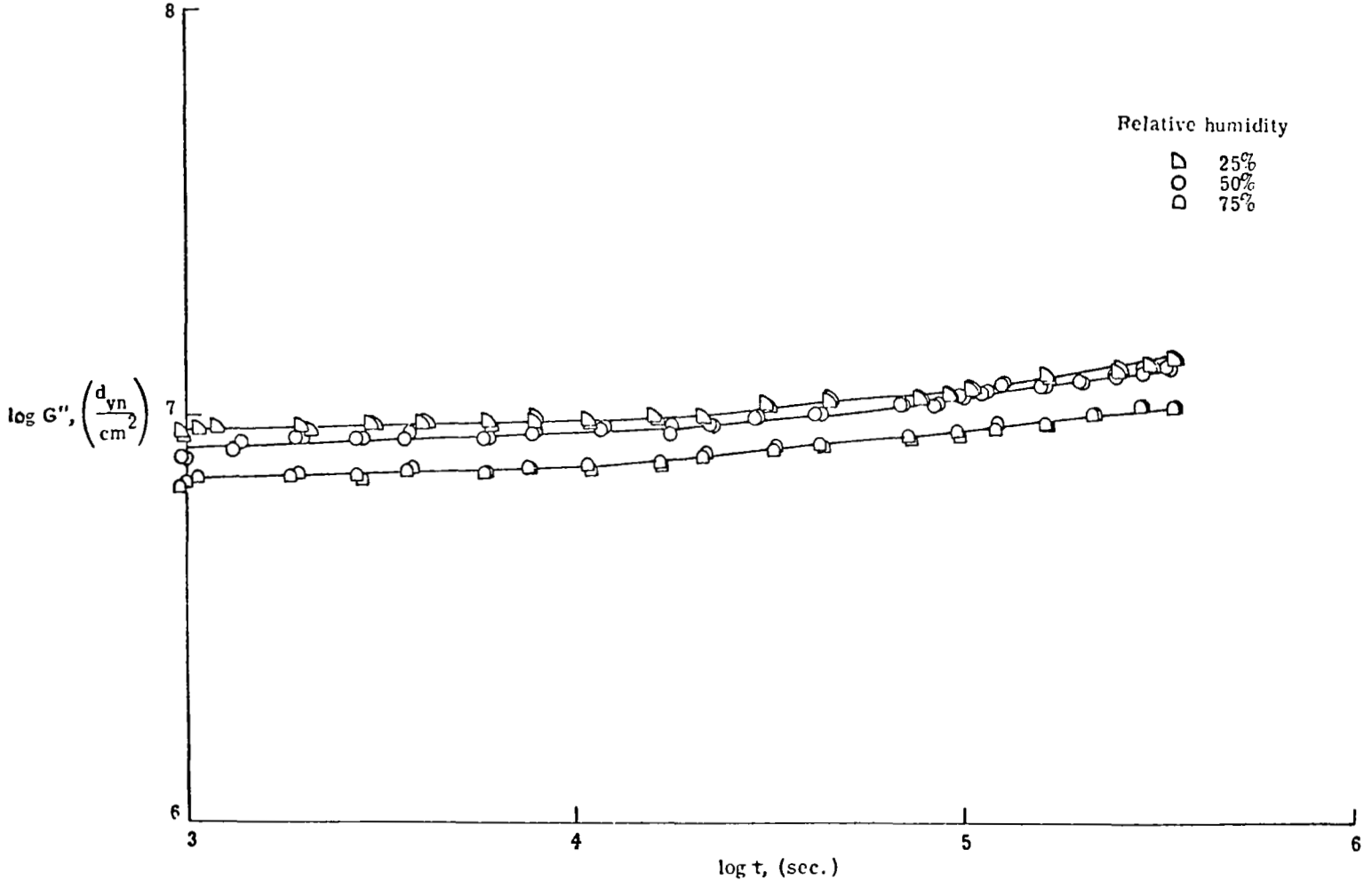

Figure 23. Preconditioning Differences Reflected in the Loss Modulus of TPH 3105 during Vacuum Exposure. All samples run at 25° C.

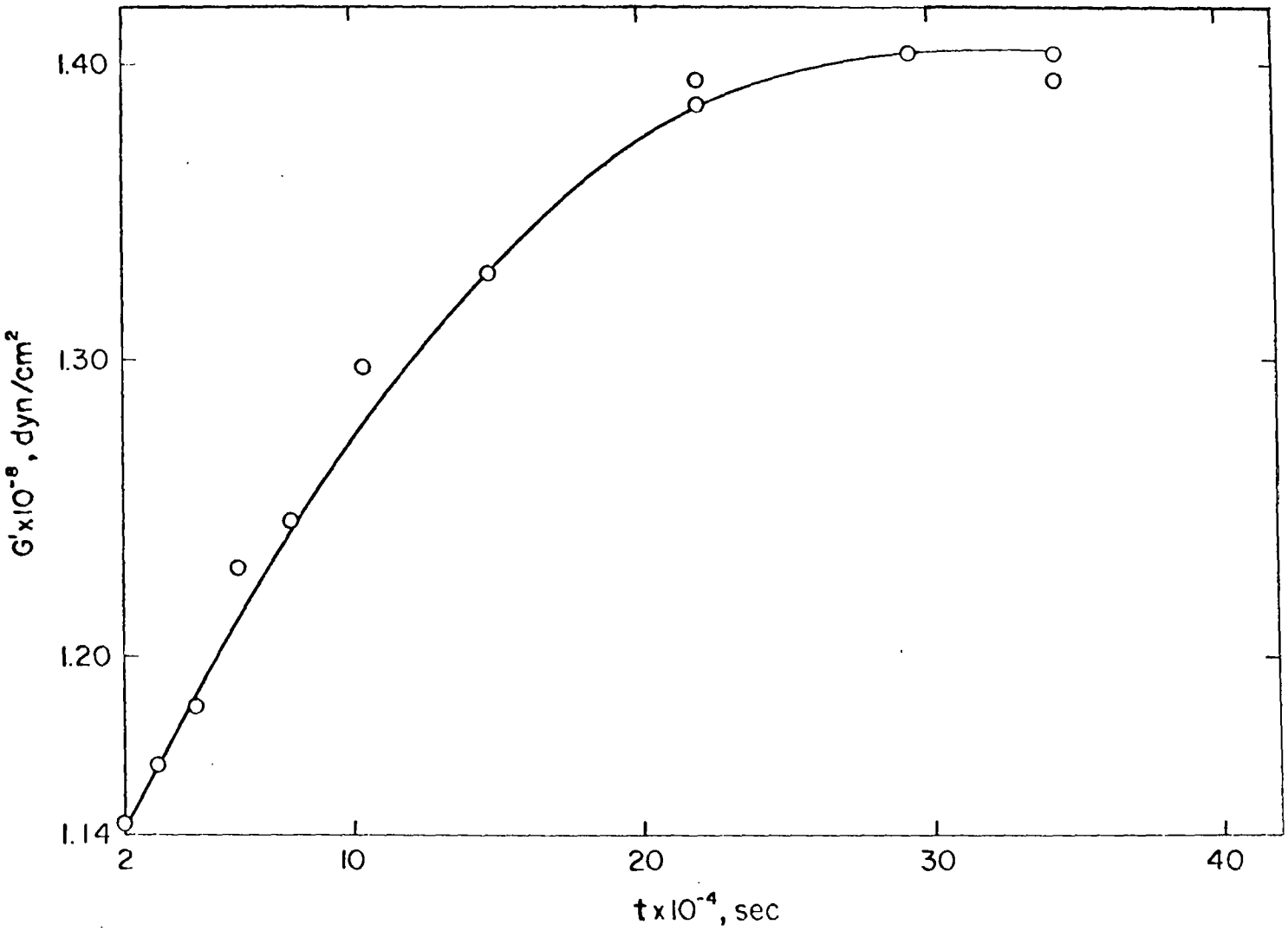

Figure 24. The Storage Modulus of TPH 3105 during the Latter Stages of Vacuum Exposure. Sample was 50% R.H. preconditioned. Plot is a 25° C isotherm.

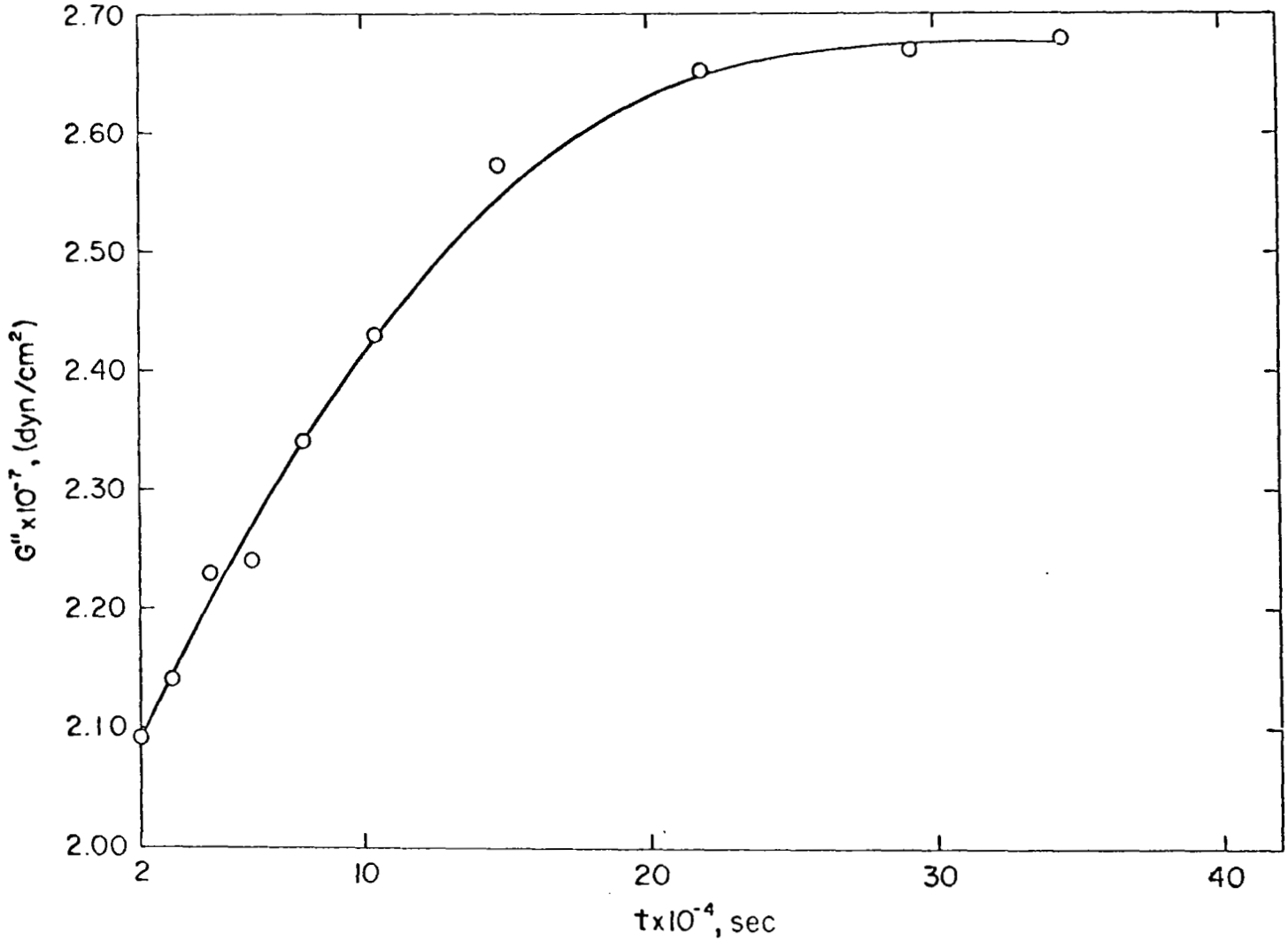

Figure 25. The Loss Modulus of TPH 3105 during the Latter Stages of Vacuum Exposure. Sample 50% R.H. preconditioned. Plot is a 25° C isotherm.

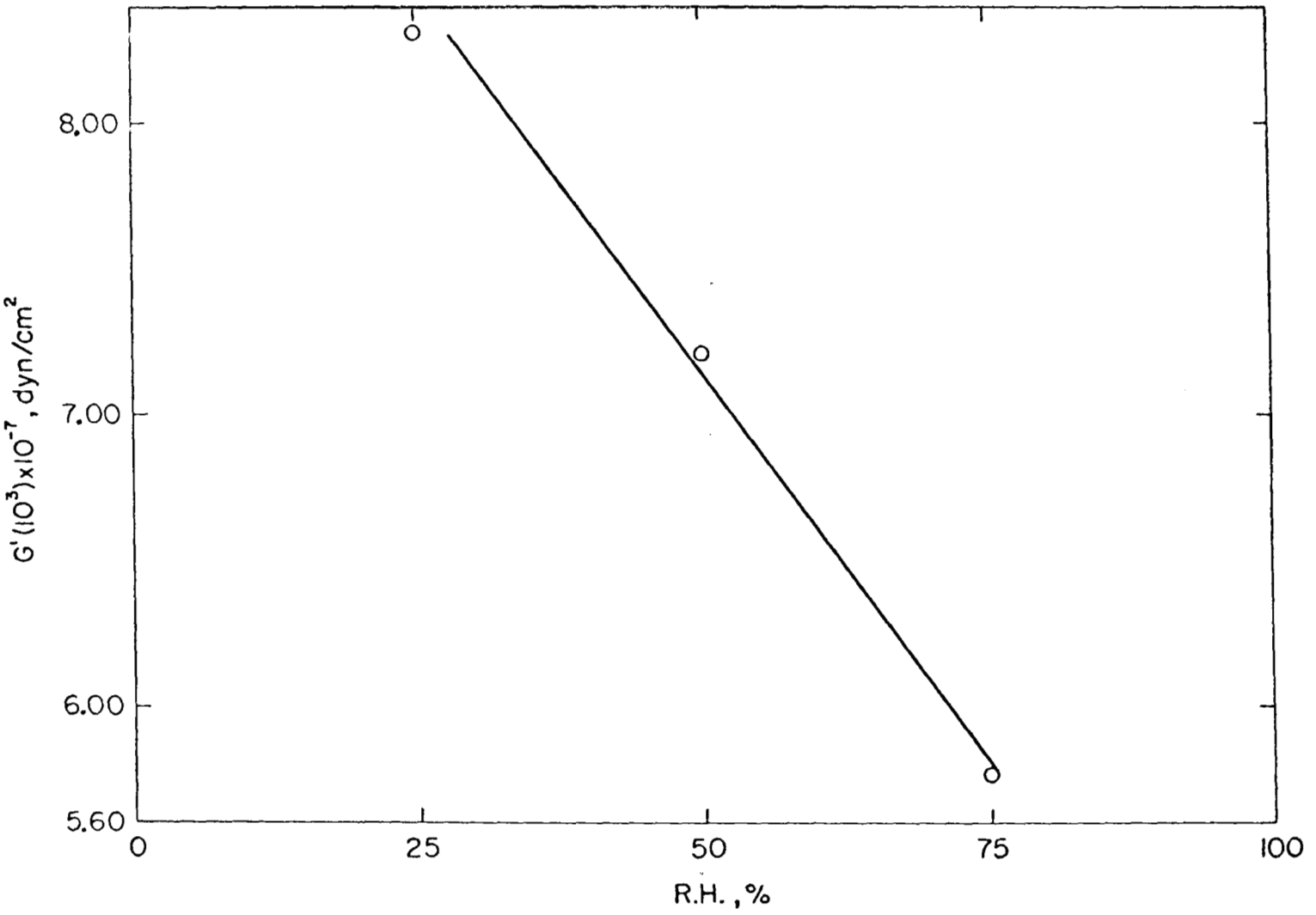

Figure 26. Preconditioning Effects on the TPH 3105 Storage Modulus after 1000 Seconds Vacuum Exposure. Plot is a 25° C isotherm.

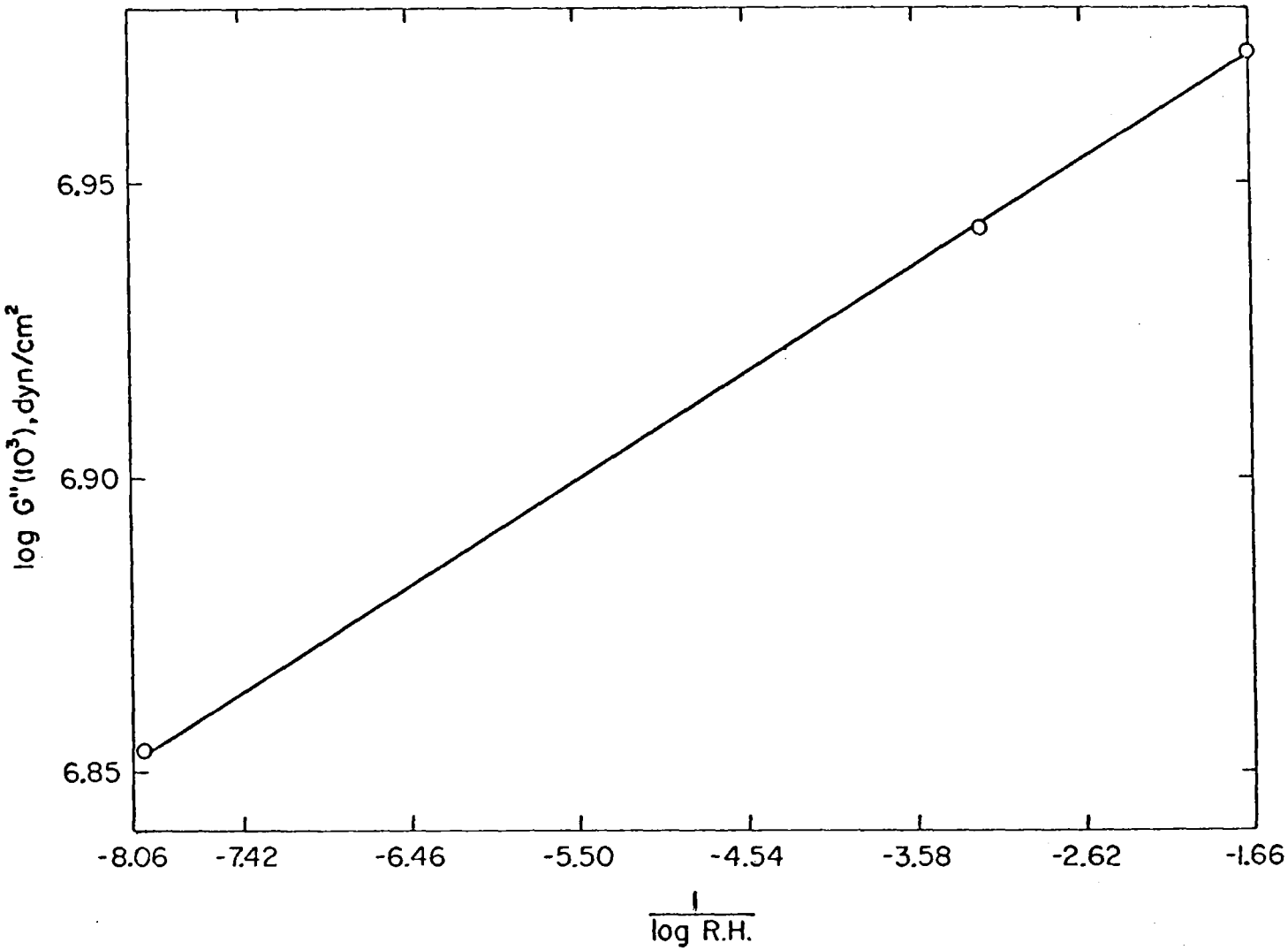

Figure 27. Preconditioning Effects on the TPH 3105 Loss Modulus after 1000 Seconds Vacuum Exposure. Plot is a 25° C isotherm.

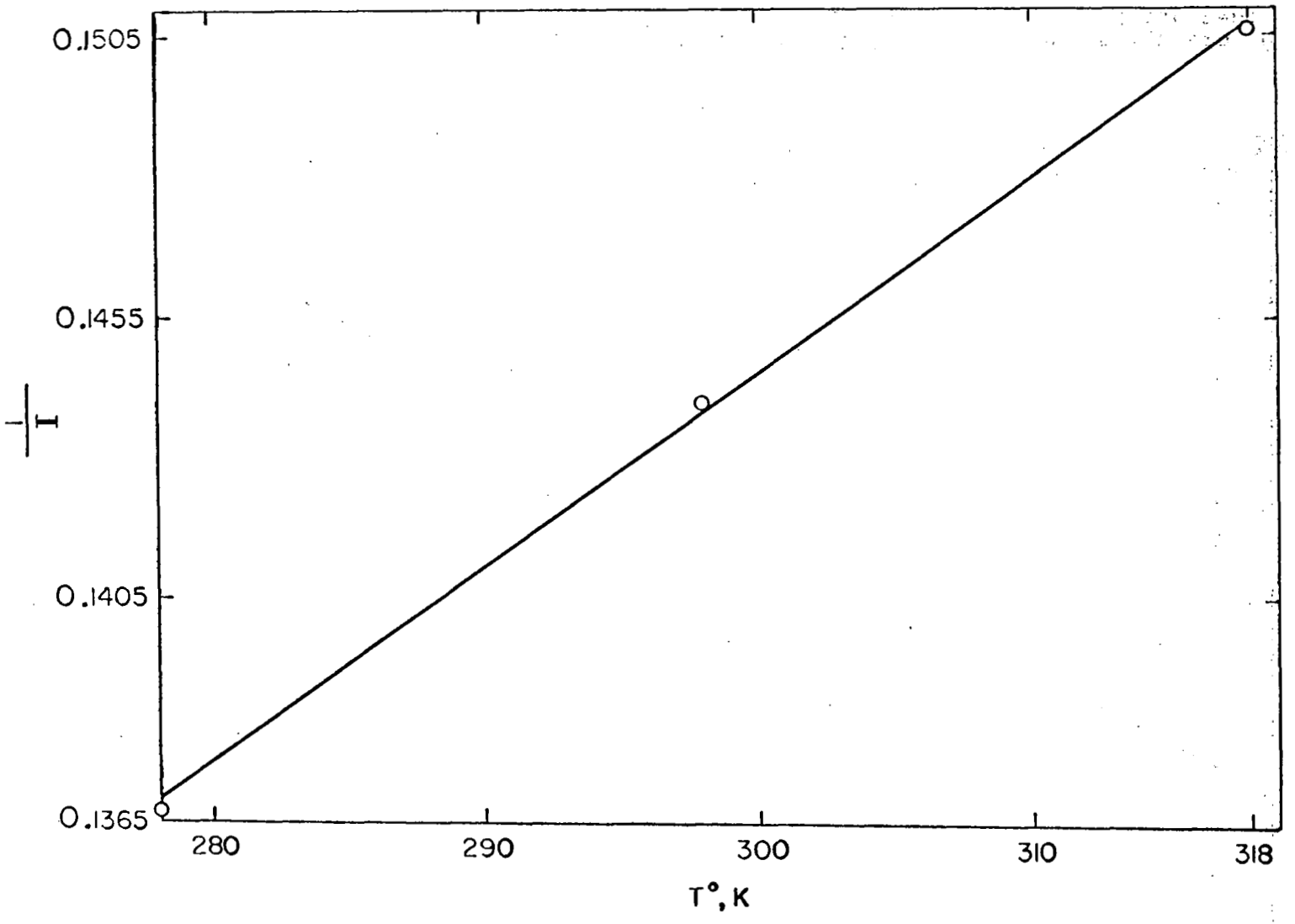

Figure 28. Influence of Temperature on the "I" Parameter of Equation 6 for the Loss Modulus of TPH 3105. Preconditioning R.H. held constant at 50% for all samples.

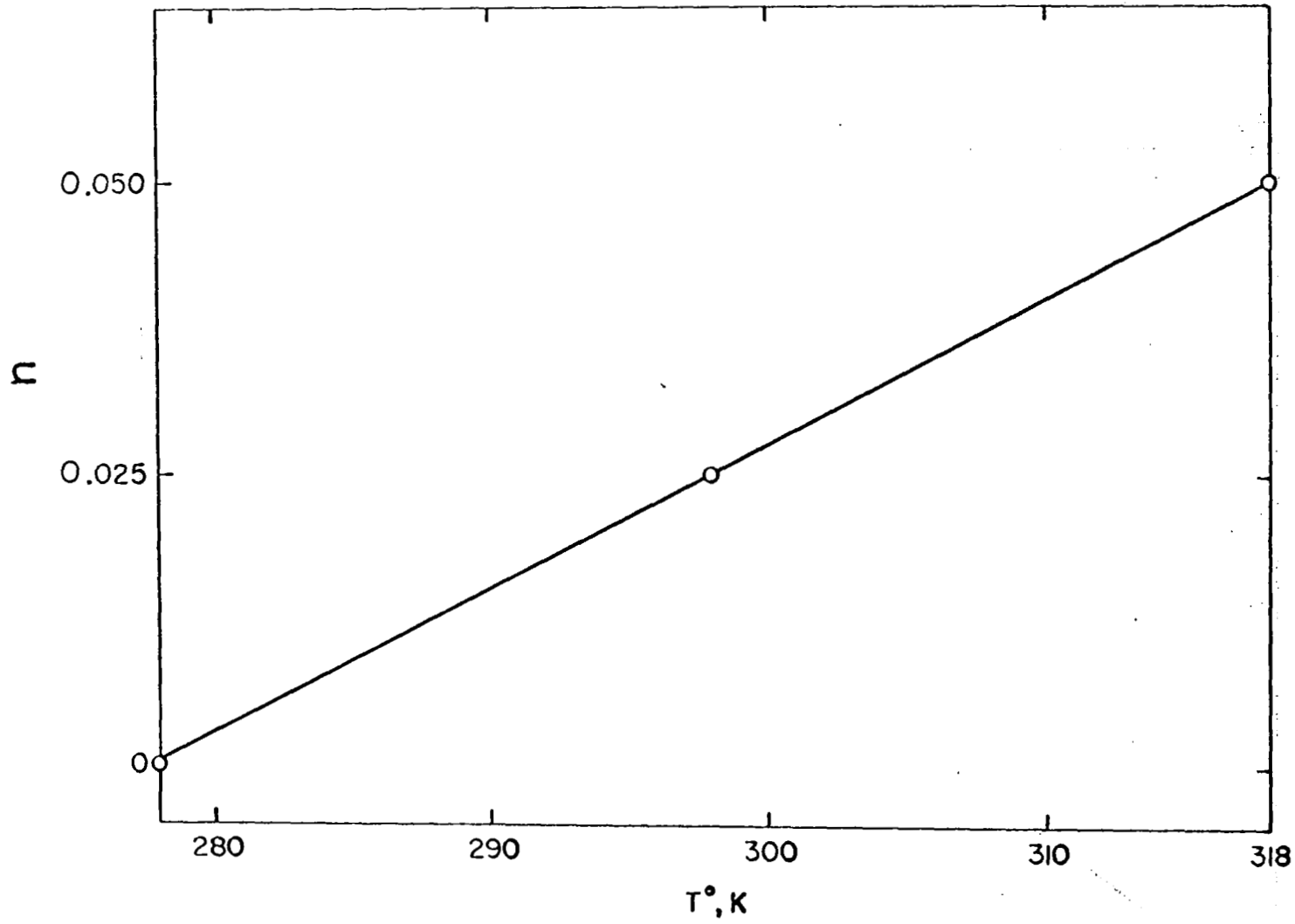

Figure 29. Influence of Temperature on the "n" Parameter of Equation 6 for the Loss Modulus of TPH 3105. Preconditioning R.H. held constant at 50% for all samples.

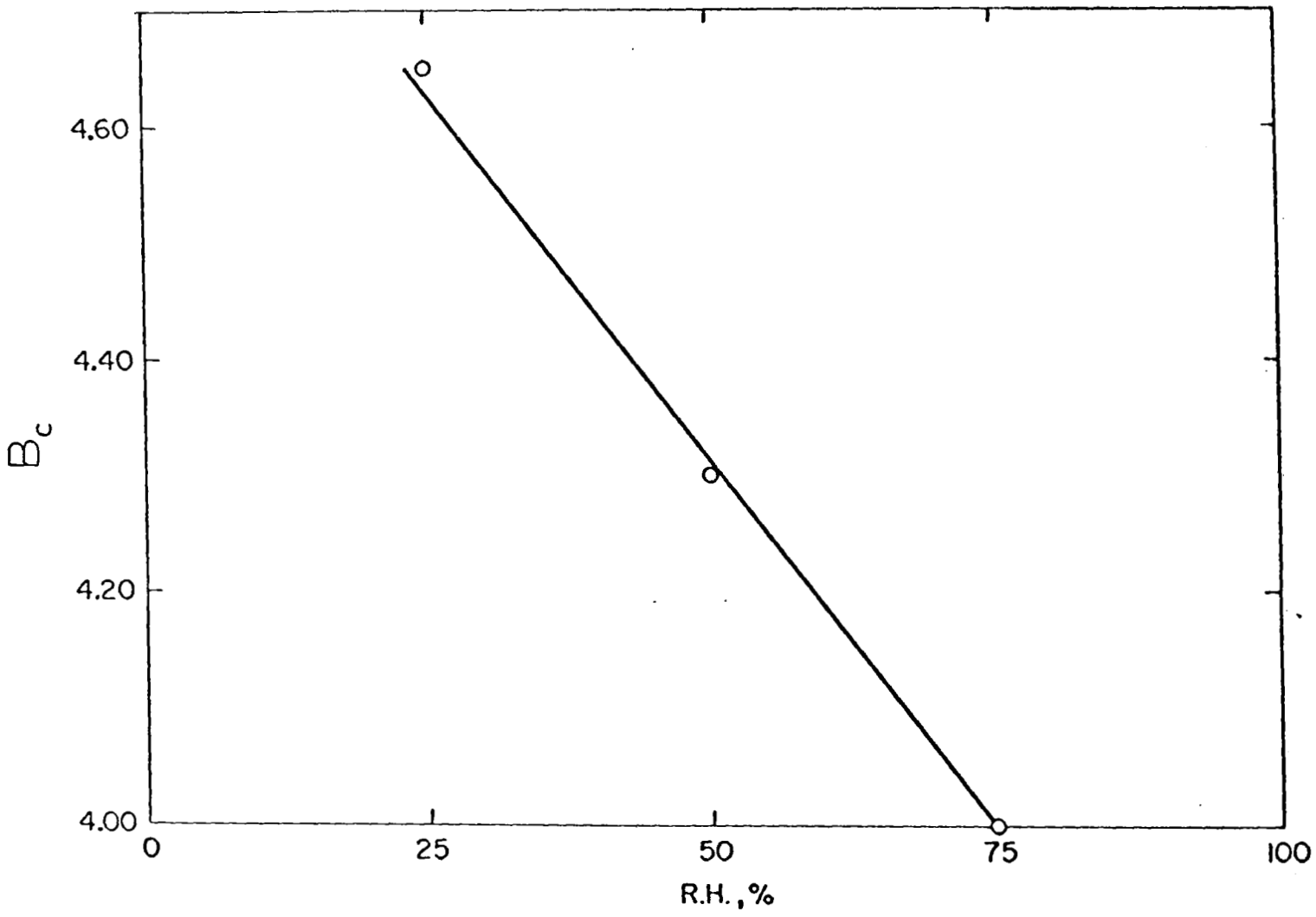

Figure 30. Influence of R.H. on the "B_c" Parameter of Equation 6 for the Storage Modulus of TPH 3105. Temperature held constant at 25° C for all samples.